Form Perception and Neural Feedback: Insights from V1 and V2

Rhiannon Jeans

Supervisor: Dr. Andrew Charles James

Submitted in partial fulfilment of the requirements for the Honours program in Psychology in the Research School of Psychology, The Australian National University.

October 2014

Word length: 11,998 words

Please note that the Acknowledgements have been altered in order to protect confidentiality

Acknowledgements

My decision to do honours in psychology over neuroscience was among many things an attempt to merge two disciplines I focused on heavily during my Bachelor degree. I believe my thesis is an example of what interesting new insights and paradigms can be developed through integrating the psychology and neuroscience literature.

To properly acknowledge the work put into this thesis, I must first thank my supervisor, Dr Andrew James. Without Andrew's technical expertise I would have messy experiment code, no good-quality processed or analysed data, and essentially no thesis to speak of. The paradigm developed for this thesis was a joint effort, with the surround line and square stimuli to control for horizontal connections to the receptive field my unique invention (you'll understand what this means if you read the thesis). I also thank Andrew for his many insights into the field of neuroscience, as well as the study of consciousness of which we have a shared interest.

Secondly, I thank Dr Deborah Apthorp for acting as advisor on this thesis and for taking me on as a summer scholar late 2013. The experience helped guide my decision to pursue a neuroimaging honours project. I also thank Deborah for her helpful advice on drafts of the thesis, particularly regarding making the neuroscience clearer to a general audience.

Thirdly, I thank Xin-Lin Goh whose source model figures I extensively cited throughout my thesis.

Next I must thank my research participants, the Diagnostics for Eye Diseases lab at the John Curtin School of Medical Research for letting me use a computer all year, and the entire Research School of Psychology for not minding that I was hardly ever around. Finally, I thank my partner, friends, and family for their ongoing support, especially during the week I was recovering from having all four impacted wisdom teeth surgically removed.

Table of Contents

Please note that the Footnotes have been added in order to reference copyright permissions

Table of Tables

Table of Figures

Abstract

In the brain, every cortical inter-area feedforward projection shares a reciprocal feedback connection. Despite its pervasive nature in the brain, our understanding of the functional role of neural feedback in form perception remains incomplete, particularly in behaving animals. This problem is addressed in humans with a novel form completion paradigm. Seven subjects (5 female) had their EEG waveforms analysed using three linear models showing non-significant differences between stimulus conditions designed to produce differences by manipulating neural feedback to V1. Two of these subjects (one female), in addition to EEG waveforms, had combined magnetic resonance imaging (MRI) and functional MRI (fMRI) cortical maps that allowed anatomically close areas such as V1 and V2 to have their signals decomposed and neural feedback inferred. Differences between stimulus conditions arose once signals had been divided into V1 and V2. Significant differences ($p < .05$) for one subject in V1 and V2 suggests cortical interactions at 100ms and 350ms. This suggests the form completion paradigm has utility at investigating the influence of the V2 far receptive field surround on V1, given future given signal to noise issues are resolved.

Introduction

The primate brain is divided into several cortical and subcortical structures (Van Essen, Anderson, & Felleman, 1992). These structures are extensively connected via neural projections, and make up important processing streams within the brain. Such processing streams have a hierarchical nature, in that each subsequent area in the stream processes something new about a stimulus in the outside world. Neural feedforward connections link areas lower in this hierarchy to higher order areas, and are coupled with reciprocal feedback connections. These reciprocal and integrative processing loops are complicated, yet they appear to be vital for normal brain function (Van Essen, et al., 1992). Despite this, our understanding of the influence of neural feedback on important processes such as visual perception within behaving animals remains incomplete (Gilbert & Li, 2013).

We attempt to address this problem by investigating inter-area cortical feedback in the process of form perception, an important aspect of visual function. Therefore, it is important to introduce the reader to the functional and anatomical basis for form perception and feedback. This includes the transduction of light in the retina, and most importantly, receptive fields in the retina, the lateral geniculate nucleus (LGN) and cortex. This will be followed by a discussion on the role of the visual cortex and cortical mechanisms such as feedforward, horizontal, and feedback projections on the receptive field. After the basic neurobiology has been defined and the question of interest highlighted, the methods that will be used in this thesis will be discussed: a novel form perception task and electroencephalography (EEG) using source analysis to estimate signals in localized brain areas (Vanni, Henriksson, & James, 2005). This will be coupled with MRI and fMRI cortical mapping to infer feedback between anatomically close areas such as V1 and V2 (Ales, Carney, & Klein, 2010). We hope to investigate

the contribution of feedback between V1 and V2 to form perception, and contribute to the growing literature on this important topic.

Introduction to Cortical Processing

The cortex is hierarchical in that processing generally occurs in a serial manner, from areas that process simple inputs such as bar stimuli in V1 and V2, the first brain areas that receive input from the eyes after the LGN (Felleman & Van Essen, 1991), to areas that process higher-order or more complicated stimuli that we have expertise in (Gauthier, Tarr, Anderson, Skudlarski, & Gore, 1999) such as faces in the middle fusiform area (Kanwisher, McDermott, & Chun, 1997). Ungerleider and Desimone (1986) examined the architecture of feedforward and feedback connections between different brain regions within macaque monkeys using fluorescent dyes, and found that they are embedded within different layers or laminar of the cortex, where there are six layers in total. Specifically, feedback projections from higher-order areas tend to terminate in the supragranular and infragranular layers of lower order areas (Ungerleider & Desimone, 1986), the granular layer being concentrated deep in the cortical column and containing many granular neurons which have small cell bodies (Gray, 1961). Feedforward projections to higher order areas from these lower order regions terminate in layer IV of the cortex (Ungerleider & Desimone, 1986). These laminar-specific projections highlight how feedforward and feedback projections play distinct roles in cortical processing. This role is complicated, as they have a characteristic and consistent asymmetry across the brain between areas, which is striking given the pervasive reciprocal nature of such connections in the brain (Figure 1). In other words, not all brain regions are connected to all others, and this organization likely has important consequences brain function. An example of such function includes the processing of form stimuli.

Figure 1. Neural feedback in the cerebral cortex. Based on research on cortical connections within the macaque monkey, this is a diagram demonstrating the extensiveness, anatomical importance, and asymmetry of neural feedforward and feedback connections. Reproduced from Van Essen et al. (1992).

Form Perception

Form perception refers to the visual grouping of smaller elements that are then perceived as part of the same object. Examples of form perception tasks include the detection of three-dimensional images (Bakin, Nakayama, & Gilbert, 2000), figure-ground segmentation (Straube, Grimsen, & Fahle, 2010), texture perception

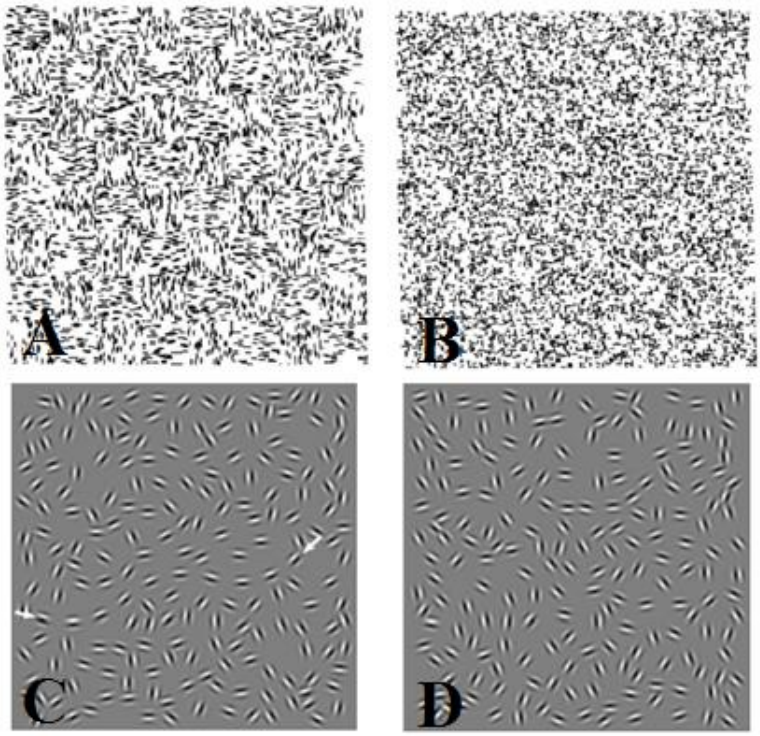

Figure 2. Examples of form discrimination displays. A) a texture stimulus, B) random texture noise, C) a contour embedded within a random background (arrows for demonstration purposes only), D) random contour background. Adapted from Lamme, Van Dijk, and Spekreijse (1992)[1] and Hess and Field (1999).[2]

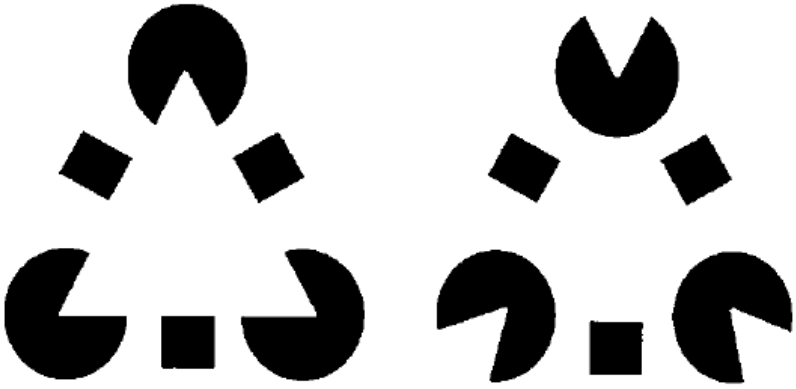

Figure 3. Example of illusory contour displays. Note the left image contains the illusory contour (a triangle) while the right one, a control condition, does not due to the orientation of the bordering elements. Adapted from Ffytche and Zeki (1996).[3]

(Lamme, et al., 1992) (Figure 2), illusory contours (Ffytche & Zeki, 1996) (Figure 3), and contour integration (Dakin & Hess, 1998; Mathes, Trenner, & Fahle, 2006) (Figure 2). One thing all these tasks have in common is that they all present the entire form display at once, usually as part of a discrimination task (for instance, identifying the interval in which a coherent "form" image appeared; see Figures 2 and 3).

The perception of form on the basis of the orientation or grouping of individual elements is termed 'element connectedness' or 'good continuation' by Gestalt psychologists, who proposed a series of rules that govern perception based on the idea that perceptual experience could not be decomposed into simple features (Hess & Field, 1999; Wagemans et al., 2012). Although this decomposition argument has been questioned in light of the new research on the complexity of brain processing (Wagemans, et al., 2012), the influence of Gestalt psychology gave rise to many of the paradigms in the form perception literature mentioned (see Figures 2 and 3). Other rules of grouping rely on features other than orientation such as like-polarity or colour ('common fate'), changes over time ('synchrony'), and enclosure within a larger object ('common region'). These Gestalt rules are thought to reflect underlying neural mechanisms of form perception (Wagemans, et al., 2012) and can guide the creation of new paradigms.

Communication between hierarchical brain regions is thought to be required to generate a Gestalt whole form percept on the basis of integration of the parts. Psychologists and neuroscientists have recognized and queried the role of feedback connections for form perception processes for over a decade (Hess & Field, 1999), and yet this issue has not been adequately addressed given the limited number of form perception studies directly looking at feedback (Mijović et al., 2014). Joint psychological and neurophysiological methods can address this issue. However, first the neural mechanisms underlying form perception must be introduced.

Introduction to Receptive Fields

Perception is the experience that accompanies a sensation; the physical interaction of a stimulus with a sensory organ. For vision, sensation begins at the retina when a light-sensitive photo-pigment absorbs a photon (aka 'light packet') within its range of spectral sensitivity (Chabre & Deterre, 1989). With enough of these events, phototransduction occurs, and a neural signal is sent to the brain via the lateral geniculate nucleus (LGN), a relay station within the thalamus between the retina and cortex.

In the retina, a receptive field (RF) is a group of retinal ganglion cells that spatially pool signals from photoreceptors and can be stimulated with an antagonistic spatial on-off configuration of light (Hubel & Wiesel, 1959) (Figure 4, left). In the retina and LGN, RFs pool information from neurons in a concentric organization, giving cell sensitivity to dot or circular stimulus in the visual field (Hubel & Wiesel, 1959; Schiller & Malpeli, 1978) (see Figure 4, left). However, in the visual cortex, RFs are sensitive to stimuli such as a central bar of a particular orientation with adjacent flanking regions (Hubel & Wiesel, 1959), and are probably formed from the spatial sum of several LGN RFs (Figure 4, right). Hubel and Wiesel (1959), in their highly influential study, found that cells in the cat visual cortex would fire to their 'preferred' orientation and bar dimension. This responsiveness to bar stimuli marks the basis of form processing in the brain. A general property of the brain is that neurons with similar response properties cluster together in columns (McLoughlin & Schiessl, 2006), thus the visual cortex is arranged into columns of orientation selectivity (Hubel & Wiesel, 1968). This gives rise to organized intra-cortical processing with RFs in each layer.

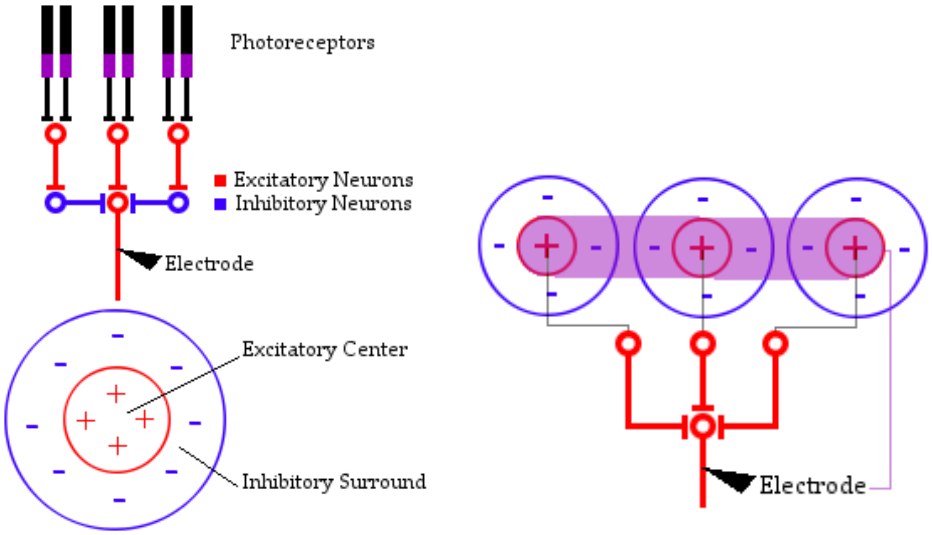

Figure 4. RF in the retina and LGN. Diagrammatic representations depicting how a RF is formed in the retina (left) and LGN (right). Adapted from Blake and Sekuler (2005) and Hubel and Wiesel (1962).

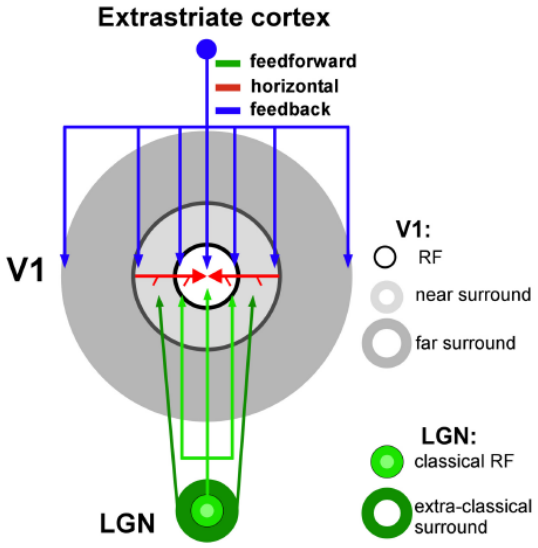

Figure 5. The extra-classical surround of a RF in V1. A recent model of RFs that proposes feedforward, horizontal, and feedback connections influence the centre, near surround, and far surround, respectively. Adapted from Shushruth et al. (2013).[4]

However, RF organization is more complicated than is implicated by a simple centre-surround model. Current research supports a model where inter-cortical feedforward connections make up the centre of the RF, intra-cortical horizontal connections influence the near-surround, and inter-cortical feedback connections influence the far surround of a RF (Angelucci & Bressloff, 2006; Angelucci & Bullier, 2003) (Figure 5).

Intra-cortical Horizontal and Inter-cortical Feedback Projections

An examination of cell-level studies is necessary to understand the neural generators of form processing, including the intricacies of intra-cortical horizontal and inter-cortical feedback signals. Horizontal connections between neurons are crudely formed before birth (Lowel & Singer, 1992), and link due to correlated activity between cells. This means multiple cells that fire to the same stimulus like a continuous border are more likely to be linked via horizontal connections than those to randomly oriented stimuli (Katz & Shatz, 1996; Lowel & Singer, 1992). Of note is that the influence of a horizontal connection on a centre cell is more pronounced once the cell is already active, than when the cell is at resting level (Hirsch & Gilbert, 1991; Weliky, Kandler, Fitzpatrick, & Katz, 1995). This highlights the fact that horizontal cells modulate activity to stimuli rather than generating their own activity in isolation of RF centre stimulation. This modulatory activity arises from single and multiple horizontal synaptic inputs (Hirsch & Gilbert, 1991) which means that a signal coding a stimulus is influenced by its surrounding elements in the visual field.

Excitatory horizontal connections exert their influence on the inhibitory RF surround based on the distance of a like-orientated visual stimulus outside the surround (McGuire, Gilbert, Rivlin, & Wiesel, 1991). Thus, horizontal connections are a key mechanism in modulating neural signals to visual stimuli based on the presence and distance of like-oriented surrounding elements. This may allow the relative position and

structure of a stimulus in the visual field to be coded within the cortex. Finally, Angelucci et al. (2002) used cell labelling in macaque V1 to highlight the extent of horizontal connections on the cortical sheet, demonstrating that there is considerable RF size variation between and within brain regions. This variation may allow the cortex to extract more information from a visual stimulus as each RF will generate new information about a given stimulus such as its size and shape. This information would then be combined to produce the most accurate signal. The contribution of neural feedback to such form processing is worth examining, as it too influences the RF surround.

Feedback connections exert a mainly suppressive effect on the centre of a RF, but can be facilitatory given the use of a low contrast instead of high contrast stimulus in the far surround (Angelucci & Bressloff, 2006). In addition, as feedback can have a very early influence, beginning as early as 10ms after neural response (Hupe et al., 2001), this means the influence of feedback on the RF can come before the influence of horizontal connections (Angelucci & Bressloff, 2006).This adds another dimension to the RF as it allows the contrast of surrounding stimuli to be integrated within the cortical representation of the visual field. As with horizontal fields, the visual field extent of feedback connections on the far-surround RF within V1, V2, V3, and other regions (Angelucci et al., 2002) are varied in size within and between brain regions but are overall approximately four times larger than horizontal fields (Angelucci & Bressloff, 2006). Feedback projections may thus code more information about the relative position and structure of a stimulus than horizontal ones. Recent evidence suggests feedback projections are not as tightly orientation tuned as horizontal fields (Shushruth et al., 2013). This is an important point as it may allow broader encoding for objects such as shapes with orthogonal corners like squares, as horizontal projections can code the borders making up the square, but do not selectively integrate corners together due to

their tendency to link only to like-oriented RFs. This orientation preference difference between horizontal and feedback projections may also allow the design of a novel visual stimulus which can selectively tap feedback mechanisms while controlling for horizontal projections.

The trend for neural feedback to be less orientation-selective than feedforward projections is present in all layers of V1 (Shushruth, et al., 2013), but hypothetically exists for other visual cortical areas as well. This broader orientation tuning gives neural feedback a unique role in providing information to the RF about how to integrate orthogonal visual stimuli. It also presents V1 as a potential target for measuring differences between horizontal and feedback processing on the basis of orientation selectivity.

Together, horizontal and feedback signals can enhance consistent grouping of stimuli in the visual field and inhibit inconsistent grouping, based on the strength of RF centre excitation, relative to the level of inhibition in the RF surround (Francis & Grossberg, 1996). Given that higher-order areas are selective for more complicated stimuli, such as the selectivity for corners and non-linear curves shown in V4 (Yau, Pasupathy, Brincat, & Connor, 2013), this makes the functional role of RF surrounds increasingly complicated when feedback signals from multiple cortical areas are to be combined (Angelucci & Bressloff, 2006; Yau, et al., 2013). Despite my earlier conjecture, the role of such feedback connections for conscious perception of visual stimuli needs expanding (Gilbert & Li, 2013), though I have outlined plausible roles for these mechanisms. This lack of understanding of neural feedback and the joint role of feedback and horizontal processing for conscious perception can be addressed by using neuroimaging methods such as EEG in human subjects, coupled with source analysis and a novel visual task. The visual task could isolate feedback projections by controlling for horizontal connections, perhaps through the manipulation of stimulus orientation.

Neural feedback can be inferred by using source analysis, which mathematically decomposes an EEG signal into the waveforms of individual generators such as different brain regions (Michel & Murray, 2012). The details of this will be discussed subsequently, but first an examination of the basis for EEG and source analysis may inform the current study concerning potential neural generators involved in form perception.

EEG and Source Analysis

EEG is a neurophysiological method that involves the non-invasive placement of metal-coated electrodes in close proximity to the scalp to measure extracellular electrical changes that reach the surface (Pizzagalli, 2007). The resulting EEG waveform is a combination of many electrical currents that reach the scalp resulting in the appearance of positive and negative peaks in the waveform. The generators of these peaks are ambiguous due to signal summation , current cancellation due to cortical folding (Ahlfors et al., 2010), the attenuation of neural currents by the scalp (Ary, Klein, & Fender, 1981; Rush & Driscoll, 1968), and because deep currents are difficult to estimate as they may represent global underlying activity over several areas (Lopes da Silva, 2004). However, EEG's greatest strength is its millisecond temporal resolution which makes it well-suited to studying the dynamic progression of neural activity (Light et al., 2010) and can make it a powerful neuroimaging tool in conjunction with source analysis techniques (Michel & Murray, 2012).

Source analysis is a mathematical technique that can be used in EEG or magnetoencephalography (MEG) to decompose the contribution of several brain areas to the post-synaptic potentials that are summed at the scalp, and hence to map the observed scalp potentials back to the underlying neural activity (Lopes da Silva, 2004). The activity that gives rise to the EGG waveforms include excitatory post-synaptic potentials that start at pyramidal neuron apical dendrites (Figure 6, left). Pyramidal neurons make

up 70-85% of the cortical neuron population and are so-named due to their cell body morphology which is triangular (DeFelipe & Fariñas, 1992). These excitatory post-synaptic potentials cause current from the extracellular space to go into the pyramidal neuron (a 'sink') which then travel to the cell body where current exits the neuron and moves into the extracellular space (a 'source') (Figure 6, left). A dipole can be taken to be a summary of extracellular potentials of a patch of cortical matter containing approximately 100,000 pyramidal cells oriented in parallel to each other and activated simultaneously (Pizzagalli, 2007) (Figure 6, right). Surface potentials on the scalp detected by the EEG thus arise due to these dipoles. The orientation of the dipole within the cortical sheet determines the polarity, and its distance to the scalp and number of neurons recruited determines the observed amplitude (Pizzagalli, 2007).

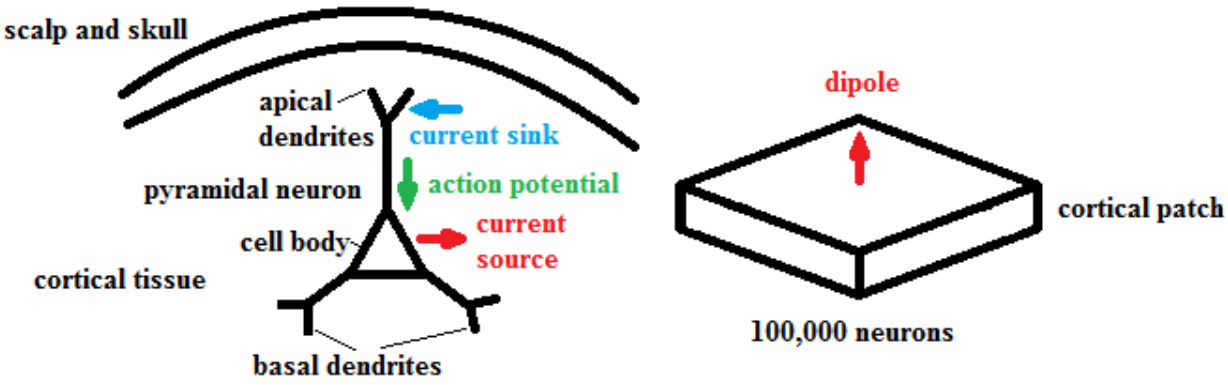

Figure 6. EEG sources, sinks and dipoles. Extracellular current entering the cell is denoted a 'current sink' and occurs at the beginning of the action potential. Once the action potential reaches the cell body and exits via the basal dendrites, the intracellular current exiting the cell is termed a 'current source'. The scalp and skull include also the meninges and cerebrospinal fluid but for simplicity have been omitted.

We assume EEG signals originate from different brain areas, and the forward model that predicts observed potentials produced by dipole sources can be estimated with numerical models (Cuffin et al., 1991).

Source analysis is influenced by choice of head model: if a subject's MRI image makes up the head model, the estimation of structures being segmented, such as the skull, meninges, ventricles, or gray matter can influence the precision of source estimates – the more structures being estimated, the better the fit (Dogdas, Shattuck, & Leahy, 2005; Ramon, Schimpf, & Haueisen, 2006). The use of a MRI image can improve the precision of source analysis and waveform generator localization from an average error of 10-30mm with a spherical source model, to 2-3mm. This was pragmatically demonstrated in a series of experiments on epileptic patients whose EEG potentials, generated manually by stimulating electrodes in the brain, had pre-defined origin (Cuffin, 1998; Cuffin, et al., 1991), allowing a direct comparison between the source current estimate and the actual source location. Source analysis has been applied to several visual perception tasks with varying degrees of success. Such examples are examined subsequently within a review of the EEG peaks underlying form perception tasks.

The most promising temporal EEG peak or component for neural feedback on form perception tasks comes from one study using the contour integration paradigm, a type of form perception task using bar stimuli oriented to produce contours (Machilsen, Novitskiy, Vancleef, & Wagemans, 2011). Machilsen et al. (2011) described a positive peak at around 100ms after stimulus presentation which they termed the P1(Machilsen, et al., 2011).They report the P1 component being sensitive to the orientation of the background containing the contour: when background elements all had the same orientation, the P1 component had a larger amplitude compared to trials where there were randomly oriented background elements (Machilsen, et al., 2011). As models of

feedback suggest that its function is in part to inhibit noise (of a background) and enhance the signal to structure (like-oriented elements) (Dura-Bernal, Wennekers, & Denham, 2011, 2012), the model suggests the P1 may have a feedback component. Source analysis techniques have localized the contour-related P1 component to dorsal occipital areas and the posterior fusiform gyrus (Luck, Woodman, & Vogel, 2000), supporting a role for interactions between several areas. Recent unpublished research on illusory contours from this lab describes a feedback projection from V2 to V1 that contributes to the P1 (Diaz, 2013), which suggests the case might be similar in the current study. Overall, the contour-related P1 could be generated by the processing involved in several possible feedback pathways, including V1 and V2.

The first occurring negative peak Mathes et al. termed the N1, at 150ms, shows significant differences between aligned and misaligned contours (Mathes, et al., 2006) and is a second, though less certain candidate for a neural feedback component. The N1 may be related to the localization of the image in the visual field, as suggested by Di Russo et al. (2002), though it could also be due to specific aspects of form; performance on a form discrimination task decreases when V1/V2 processing is disrupted by transcranial magnetic stimulation (TMS) applied at 150ms (Wokke, Vandenbroucke, Scholte, & Lamme, 2012). If there is a feedback process at P1, it does not rule out a second feedback process at the N1. Research should then aim to elucidate the timing of neural feedback between the early visual cortices.

The final discussed peak has evidence to suggest it is involved with feedback related to form perception. A peak that appears at 290ms has been reported to involve feedback process from the lateral occipital cortex (LOC) to V1 and V2 in a contour integration task (Mijović, et al., 2014), possibly related to Mathes et al.'s contour-related P3 at 300ms (Mathes, et al., 2006). V1 and V2 were confirmed to respond to the contour display in Mijović et al.'s (2014) study throughout each peak including the P3, but

feedback was not investigated perhaps due to the region's anatomical proximity. The P3 is thought to have many other non-visual generators (Herrmann & Knight, 2001; Johnson, 1993), though overall there is evidence to suggest V1 and V2 play a prominent role in form processing over time with late-feedback from the LOC.

Thus, EEG research on the neural generators of form perception has yielded some insights on what brain regions are involved, with the P1, N1, and P3 being possible candidates for interactions between V1 and V2. However, the form perception tasks used typically aim to isolate a form perception mechanism by comparing detection of a display with randomly-arranged elements and a figure embedded, versus one with no figure or one that is disrupted (Wagemans, et al., 2012). In other words, it presents a stimulus to the entire visual field. This lack of control over stimulus display can render source estimates ambiguous and unreliable, particularly when the visually stimulated regions are close together (Hagler et al., 2009). In other words, the presentation of entire and diverse form displays does not isolate the role of individual RFs but convolutes the signals from many, which results in many dipoles of different orientations contributing to a waveform, something EEG is sensitive to (Ahlfors, Han, Belliveau, & Hämäläinen, 2010). This also brings into question the findings of many form perception EEG studies and the waveform differences associated with the comparison between two conditions, particularly when different oriented dipoles are being activated; to what degree do these differences reflect changes in the display versus reflecting controlled form perception mechanisms? Unfortunately, due to the diversity of paradigms in the form perception literature and the limited EEG studies on the subject, there is considerable variability between paradigms regarding which peaks are reported as significant, perhaps partially due to this lack of stimulus control. I have summarized the peaks most prominently reported as significant, though this diversity highlights a need to approach new paradigms in an exploratory manner.

This source estimation and stimulus control problem can be solved by isolating a signal to a single region on the cortical sheet, by presenting a stimulus to an isolated region of the visual field. This may allow RF modulation to be targeted if the stimulus appears within a larger continuous stimulus already present, something Gestalt psychologists might call an example of 'common region' (Wagemans, et al., 2012). A separate recording produced by stimulating many different isolated regions can then produce a subject's retinotopic map, where stimuli presented to specific visual field regions produce activity which can map onto relative positions on the cortical sheet and provide associated waveforms (Hagler, et al., 2009). This maps the upper and lower halves of the visual field to lower and upper cortex positions respectively, and the left and right halves to contralateral positions on the cortical sheet (Clark, Fan, & Hillyard, 1994). This practice can constrain source estimates (Hagler, et al., 2009). A retinotopic map can be obtained based on multiple region stimulation or multifocal stimulation of the visual field, usually with a circular dartboard stimulus (Figure 7), and then by recording the regions stimulated on the cortical sheet with fMRI, which is then mapped to a high resolution MRI image (Vanni, et al., 2005) (Figure 8).

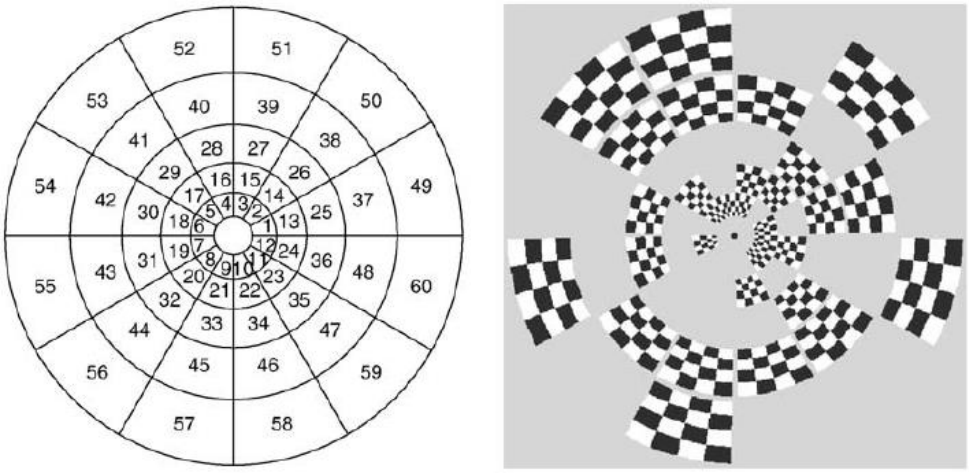

Figure 7. Circular multifocal dartboard stimulus. A circular dartboard stimulus (right) and the 60 regions it stimulates (left) used for retinotopic mapping of the visual cortex. Adapted from Vanni et al. (2005).[5]

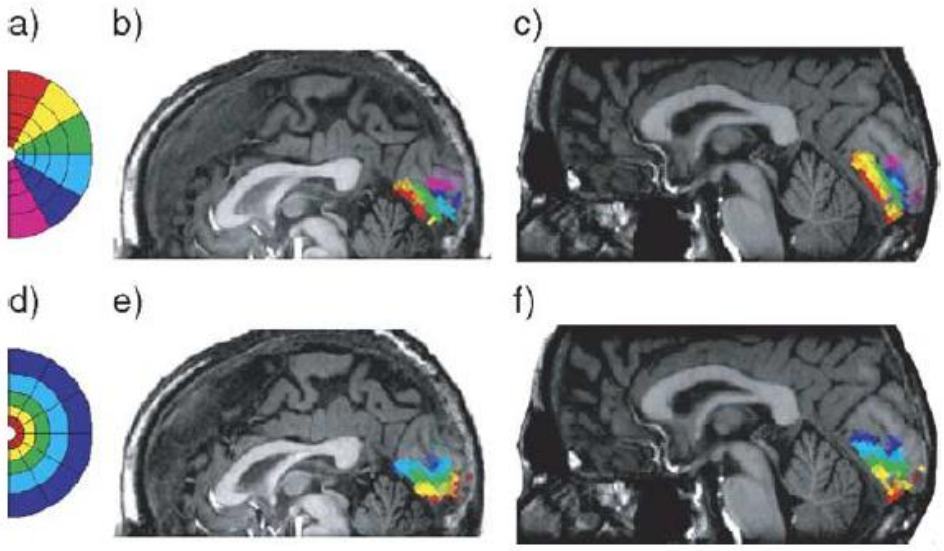

Figure 8. Retinotopic mapping from fMRI activated regions onto an MRI image. Colour coding is given for the polar angle and eccentricity (distance from central vision) of the visual stimulus (a) and (d) and the resulting mapping onto two different subjects (b),(e), and (c), (f) . Adapted from Vanni et al. (2005).[5]

While the LOC and other brain regions have been shown to be involved in form perception, less is known about the role of feedback from V2 to V1 due to their anatomical proximity, which makes them difficult to estimate. A method that utilized fMRI retinotopic maps coupled with MRI images of a given subject would be well suited to tackling this problem, and would allow inferences of feedback to be clear due to the increase in stimulus control and cortical resolution. Therefore, the current work aims to contribute to the form perception literature by quantifying the temporal progression of V2 to V1 feedback by attempting to control for such confounds. Why V1 and V2 might be so prominently involved in early visual processing is discussed subsequently with reference to their anatomical organization.

Anatomical and Functional Architecture of V1 and V2

V1 and V2 are located at the dorsal medial portion of the cortex and the anatomical extent of each region varies between individuals (Amunts, Malikovic, Mohlberg, Schormann, & Zilles, 2000) (Figure 9).

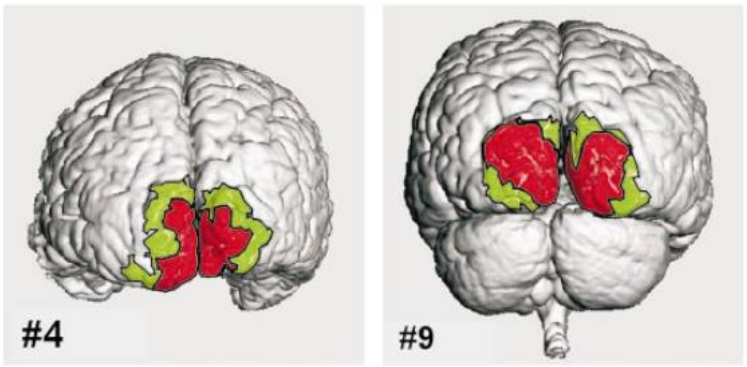

Figure 9. Example location and variation in two subjects of and V2. V1 is in red and V2 is in green Adapted from Amunts et al. (2000).[6]

LGN signals to V1 include the parvo-, magno-, and konio-cell pathways (Chatterjee & Callaway, 2003), which convey information about motion, colour, and

form from cells in the retina that are selective for those stimuli (Chatterjee & Callaway, 2003; Ölveczky, Baccus, & Meister, 2003). These distinct stimulus-carrying pathways influence how signals are organized in V1 and V2 (Sincich & Horton, 2005), as the cortex tends to organize neurons with similar response properties into columns (McLoughlin & Schiessl, 2006). When V1 is stained with cytochrome oxidase (CO) in macaque monkeys, two major cell regions become apparent: the patch and inter-patch region (Sincich & Horton, 2002) (Figure 10). Although an oversimplification, the patch regions process colour and the inter-patch region process form and motion stimuli (Sincich & Horton, 2005), suggesting the presence of distinct anatomically-defined streams.

These distinct processing streams in the brain are preserved from V1 to V2 where CO staining reveals thick, thin, and pale stripes in V2 that are selective for motion, colour, and form respectively (Sincich & Horton, 2002; Sincich, Jocson, & Horton, 2010) (Figures 10 and 11).

Figure 10. Cytochrome oxidase staining of V1 and V2. In V1 the patch and inter-patch region is visible, the cytochrome oxidase staining the patch region. The curly brackets highlight the thick stripes in V2, the black arrows point to the thin stripes, and the clear space in between denotes pale stripes. Adapted from Sincich and Horton (2002).

Images have been removed for copyright reasons

Figure 11. Laminar origin and stripe projections from V1 to V2. An illustration demonstrating the connections between V1 and V2 patches and stripes. Adapted from Sincich and Horton (2002).

However, these streams in V1 and V2 are not completely segregated and interactions occur as evidenced by the presence of neurons in V1 and V2 that are selective for multiple stimulus types such as form and colour (Roe, 2011; Roe & Daniel, 1999). It is worth noting that the RFs in pale and thick stripes unique to V2 may have different tuning properties suggesting a local V2 network is influencing this difference rather than the preservation of V1 laminar and compartmentalization (Sincich, et al., 2010). This reinforces the idea that at each successive stage in the processing stream, more information is extracted about a stimulus before being fed back into lower order regions. In fact, V2 appears to process one type of form stimulus that V1 does not on the basis of the organization of RFs in the pale stripes. One example of this is that 44% of 102 V2 neurons responded to an anomalous or illusory contour whereas V1, with the exception of 1 out of 60 neurons, did not (von der Heydt & Peterhans, 1989) (Figure 12).

Images have been removed for copyright reasons

Figure 12. Example of a contour and anomalous contour. Either stimulus moved back and forth 8 times at 16 different orientations covering a range of 180º. The contour (left) is a simple line. The anomalous contour (right) refers to the 'invisible' line that appears at the border of the lines. Adapted from von der Heydt and Peterhans (1989).

As subsequent visual cortices process more complicated stimuli such as complex motion in V3 and MT (Gegenfurtner, Kiper, & Levitt, 1997; Mikami, Newsome, & Wurtz, 1986), and form in V4 (Roe et al., 2012), recurring interactions between V1 and V2 may be important for processing the basic form features of a stimulus. This idea of time-dependent feature-processing has been supported most notably by studies where V1 and other cortical areas were functionally and non-invasively disrupted with TMS at different time points, and the negative consequences of this for visual perception were quantified (de Graaf & Sack, 2014; Wokke, et al., 2012). V1 and V2 therefore have an important role in form processing and the temporal contribution of neural feedback to form perception will be examined.

The Current Study

There are several different types of form perception tasks available to use for any given experiment. I propose the use of a novel form perception task, coupled with EEG and source analysis, with MRI and fMRI cortical maps for improving the precision of

the V1 and V2 source estimates. EEG and source analysis have been used to make inferences about neural feedback in human subjects previously (Diaz, 2013; Mijović, et al., 2014), so the current study can contribute to an existing literature. In this literature, the role of feedback between V1 and V2 has been established but the precise temporal contribution of feedback within a controlled design needs elucidating.

To control stimulus presentation to a point where feedback can be reliably inferred, a novel approach is required. I propose to present a single part of a form stimulus at a time to fill in a larger stimulus already present on the display. I call it a form completion paradigm. This reduces the amount of masking by neural signals from the surround associated with presenting the entire form display at once, allows a high resolution source analysis to be performed, and might allow the horizontal connection modulations of RFs to be controlled.

The latter might be accomplished by comparing the response to a single element that makes up a line surround stimulus versus a surround square stimulus on the basis of the extremely reduced influence of horizontal connections at 90º of orientation (Shushruth, et al., 2013). This may allow the modulation of the smaller bar by the surround (line or square) to be measured and perhaps horizontal and feedback processes distinguished on the basis of their differing orientation selectivity (Figure 13 and 14).

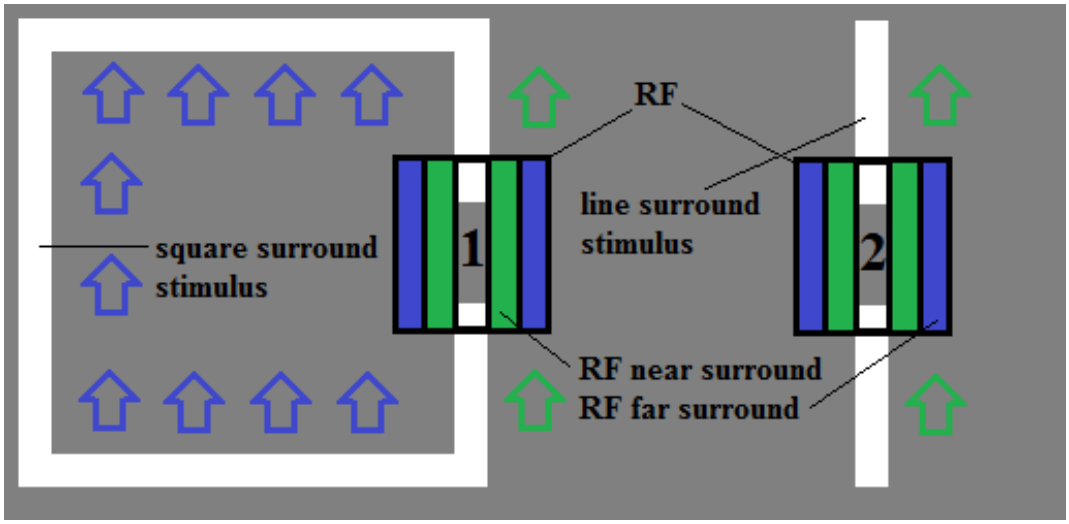

Figure 13. Square and line surround stimuli and RF modulations. The RF is a diagrammatic representation of a V1 bar-selective RF. If a smaller bar appears in the centre of RF (1) while the white square surround stimulus is present, that surround may elicit more feedback modulations on the far surround of the RF than in (2) where no such borders exist. The arrows represent relative activation of the suppressive horizontal (green) and feedback (purple) projections. Feedback arrows elicited by the main border has been omitted for simplicity, as have horizontal arrows to the surround square borders.

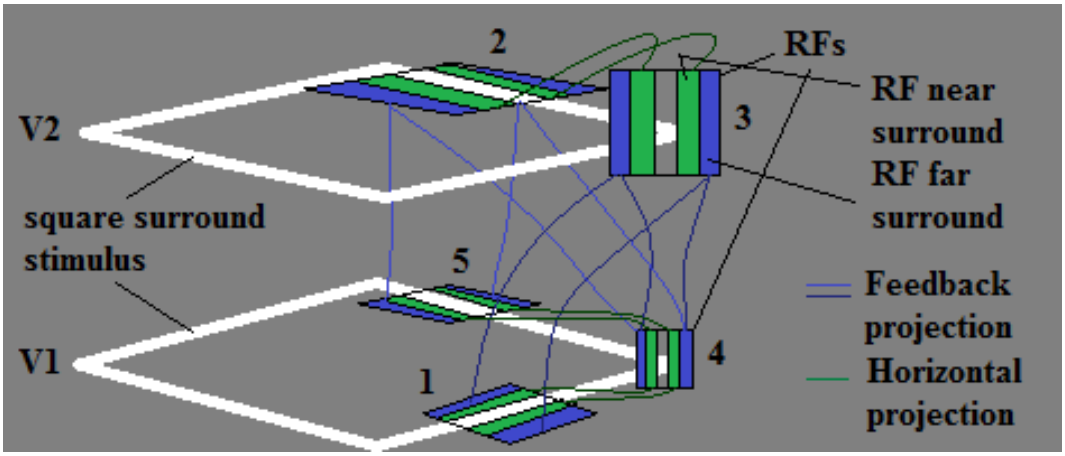

Figure 14. Diagrammatic representation of feedback to square surround stimulus. If the stimulus appears at (1), possible modulations to the RF might come from feedback from RF (2) and (3) where the latter are oriented across a corner (not aligned or orthogonal to it). (4) might be weakly linked via horizontal connections to (1) and (5), as with (2) to (3). This model suggests the strongest modulation on (1) is from the feedback projections which are less orientation selective and thus carry a stronger signal than the horizontal connections which are only weakly linking the RFs.

Given feedback is less orientation selective (Shushruth, et al., 2013), the greatest contributor to a difference waveform at V1 between the element completing a form stimulus with a like-oriented (line surround) compared one that is orthogonal borders (square surround) is expected to be due to feedback.

Three potential outcomes are anticipated for the comparison between the square and line surround stimulus modulation on the smaller bar - the latter henceforth called the target. If the excitatory potentials from the feedback and horizontal projections exceed the level of inhibition on the RF surround, a larger waveform is expected to the square stimulus surround. As far-surround facilitatory effects have only been reported to low contrast stimuli thus far and this study proposes the use of a high contrast one

(Angelucci & Bressloff, 2006), stimulus contrast would be an unlikely explanation for a larger waveform.

If RF centre suppression, an inhibitory effect, is more pronounced than the excitatory potentials from the feedback projections, a smaller waveform to the square surround stimulus modulation is expected, but this is unlikely given that the number of excitatory currents from the feedback and horizontal projections are likely to outweigh the suppression on the centre (Angelucci & Bressloff, 2006).

A null hypothesis suggests no difference between the waveforms. An unlikely explanation might suggest this is because feedback is more narrowly orientation selective than previously suggested, contrary to Shushruth et al's (2013) findings in humans and macaque monkeys. Positive and negative current cancellation is possible if the near and far RF surround modulations are approximately equal to the centre-inhibition. Other explanations would suggest that the feedback and horizontal modulations on the target stimulus were too subtle to be detected or that the target was not being neurally integrated with the surround.

To test whether the target is indeed being integrated with the already-present stimulus surround, which is an assumption underlying the line and square surround manipulation, two additional conditions will be used: an orthogonal and collinear target, relative to the surround stimulus's position. Specifically, if the target is collinear the inhibitory modulations from the horizontal projections will lead to the waveform response to the target being smaller than if it were orthogonal (Figure 15), unless the excitatory response from the horizontal and feedback projections obscures this signal. If there were no difference in the waveform to the collinear or orthogonal stimulus it would suggest the line and square surround had no influence on modulating the signal. This could be as the experimental manipulation was either too subtle to produce an observable difference or the assumptions underlying the manipulation were incorrect. It

is expected to work given our understanding of horizontal and feedback projections on modulating the RF.

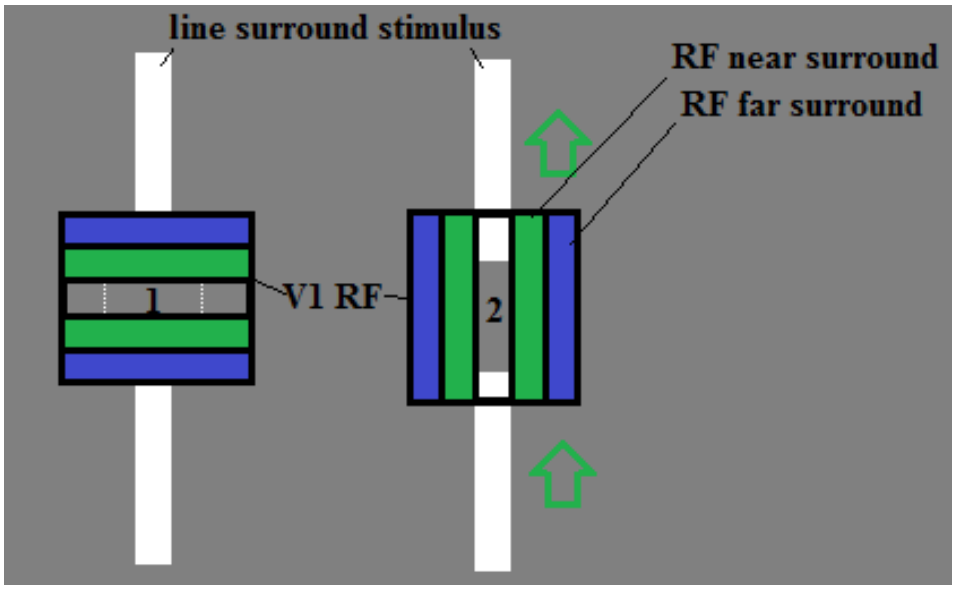

Figure 15. Collinear and orthogonal target stimulus and RF modulations. As in Figure 13, the RF (square box) is a diagrammatic representation of a V1 bar-selective RF. The green represents the horizontal connection specific RF near-surround and the purple represents the feedback specific RF far-surround. The RF is oriented orthogonal (1) or collinear (2) to represent the elicited centre RF response to a similarly oriented smaller white bar stimulus. The green arrows in (2) show that relatively more suppressive horizontal projections are acting on the RF near surround than in (1) due to the iso-orientation of the surround stimulus.

Even within recent neuroimaging studies (Shigihara & Zeki, 2014), this proposed level of display control has not been attempted, so the current study is highly useful, albeit experimental, and can elucidate the role of RFs during a form percept as well as provide information on the temporal progression of neural feedback. To infer feedback between V1 and V2, source analysis must be performed.

Finally, neural feedback can be inferred from the source estimates of contributing V1 and V2 signals thanks to EEG's high temporal resolution (Mijović, et al., 2014) and by converting the estimates into currents by transforming the signal on the basis of cortical thickness. Thus we have a way to infer feedback between V1 and V2 based on the direction of the currents, which is vital given the hypothesis of interest. It is worth noting that EEG signals in V1 and V2 are correlated with conscious perception of stimuli (Rees, 2007), so V1 and V2 make appropriate candidates for detecting dipoles associated with form perception.

In summary, I have explained the role that RFs in the retina, LGN, and cortex and the critical role RFs play in form perception. I have highlighted the complex interactions between feedforward, horizontal, and feedback connections and how they modulate the signals of oriented stimuli, including those with corners or anomalous contours. I have reviewed the literature on the neural correlates of form perception, and introduced potential manipulations to a novel task to study neural feedback. I have identified several possible occipital waveform peaks that may be associated with neural feedback from V2 to V1 that could be investigated using EEG and source analysis. These methods provide the temporal and spatial resolution necessary to estimate neural feedback between V1 and V2.

Methods

Participants

Seven subjects (5 female) were recorded and analysed for waveform differences (mean age = 28.5). Five of these subjects were undergraduate students at the Australian National University. For two of the subjects (1 female, mean age = 44) detailed source mapping information was available. These two were further analysed to infer the waveforms of current dipole density of the presumed underlying generators within V1 and V2 at the corresponding retinotopic location, thus allowing for the inference of

neural feedback. All subjects had normal or corrected-to-normal vision and no neurological disorders. For the two subjects with cortical maps, the retinotopic distributions of V1 and V2, mapped with fMRI along with the two-dimensional parametization of their cortical surface from anatomical MRI data using Brain-Suite software, was obtained previously (Goh, 2008). The participants were fully informed of all procedures and signed an informed consent form, in accordance with the ANU Ethics Committee protocol 2010/194.

Design

A Biosemi ActiveTwo (Amsterdam, The Netherlands) EEG system was used, configured in-house for 64 electrode locations. We used the 10-10 configuration system (Figure 16) with a 256Hz sampling rate. The stimulus display appeared on a 19 inch Sony Trinitron Multiscan G420 CRT monitor. The monitor extended radially from the point of fixation in the centre of the screen +/- 18.25 degrees of visual angle horizontally and +/- 13.75 degrees vertically when the subject was situated 57cm from the monitor. The stimulus background extended to a radius of +/- 17.25 degrees horizontally and +/- 12.75 degrees of eccentricity vertically, respectively. The monitor ran at 100 Hz with the background and stimulus luminance measured to approximately 50 cd/m^2 and 100 cd/m^2 at 100% contrast (Luminance of target-Luminance of background)/Luminance of background*100). Timing of stimulus appearance was tested with a photodiode to check for accurate presentation of stimulus markers within the EEG acquisition software, and was found to be within the millisecond range. This is important given the waveform of interest is bound to the stimulus.

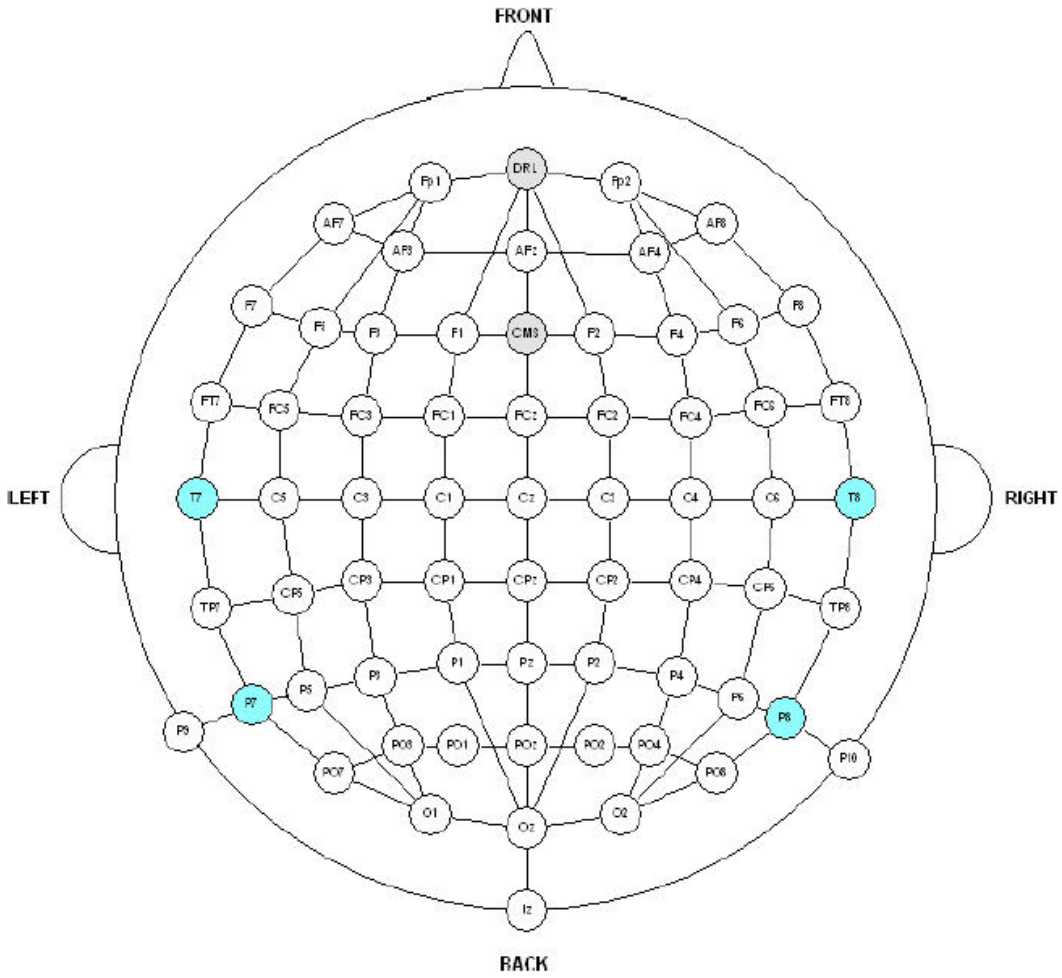

Figure 16. Electrode configuration of the 10-10 EEG system. Adapted from Goh (2008).[7]

Task

The task was written in MATLAB version 2012b using Psychtoolbox version 13.0.1 (Brainard, 1997; Kleiner et al., 2007). The task involved attentive viewing of the stimulus display followed by a two alternative forced choice (2AFC) judgment on a feature (red line) on the target being present or absent. The surround stimuli were made of continuous white bars, with a fixation cross in the centre of the screen (Figure 16). Each surround stimulus presented had a bar missing from one of its borders. During each trial, the target would pulse on and off within the already-present stimulus surround (line or square) to elicit a waveform by completing the larger stimulus (collinear) or not

completing it (orthogonal). This can be considered a 2x2x2 design. There are two possible surrounds (line vs square), two surround orientations (horizontal vs vertical, Figure 17) and two different target configurations (collinear vs orthogonal). The collinear and orthogonal stimuli appeared 9 times each (9*2=18) for each stimulus surround (x4), this sequence was repeated four times (x4) and then the entire run repeated (x2) after a five-minute break. This resulted in a total of 576 trials for each participant. Each trial, including the rest period, took approximately 2-5 seconds. As progression to the next trial was self-paced, this interval could be longer. The task took approximately 30-40 minutes to complete.

At the start of the trial, a display with the line or square surround appeared for 1000ms, to allow any signal associated with the image to dissipate (for similar tasks like contour integration, this is estimated to be around 500ms (Straube & Fahle, 2010)). There was an additional prestimulus period of between 200 and 300ms, randomly varied. The target then appeared for 80ms, short enough to prevent eye fixation movements but long enough to allow perception of form (Straube & Fahle, 2010). Whether the target appeared aligned or orthogonal was randomized. After an additional 500ms to record the waveform associated with the target, the screen went grey and the participant was prompted with white text in the lower left hand of the screen to make a 2AFC judgement (‘was the red line present or absent?’) to continue (Figure 18). The break also allowed subjects to blink if needed before continuing.

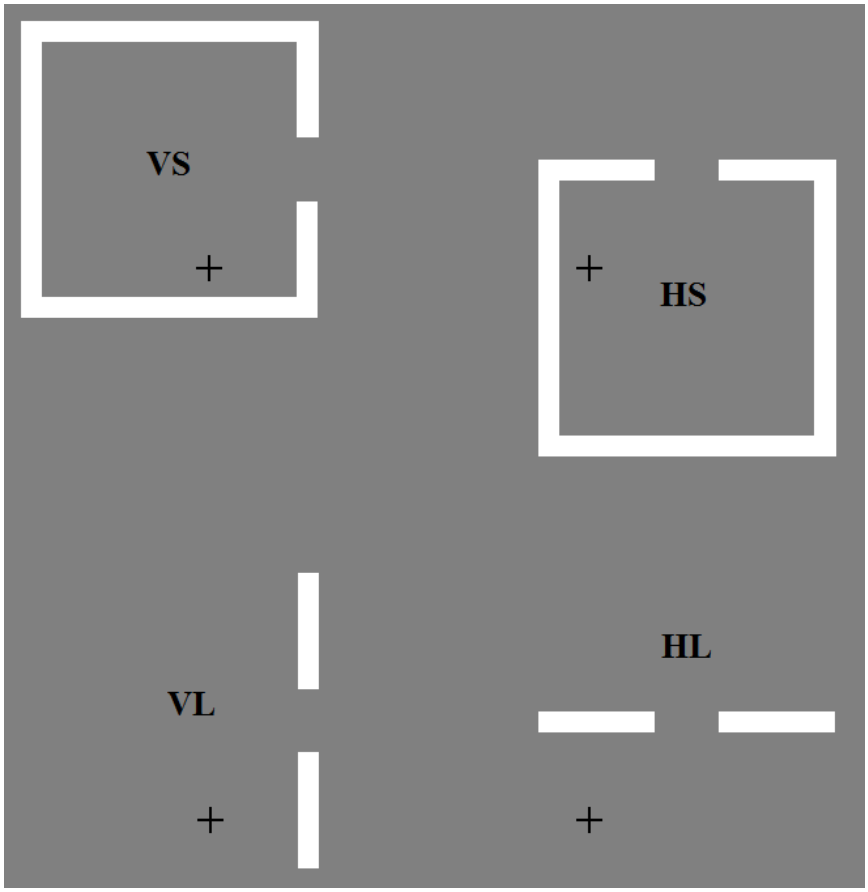

Figure 17. The four different surround stimuli. The stimuli are positioned relative to the fixation cross in the centre of the screen. The top row depicts the vertical (VS) and horizontal (HS) square surround stimuli, and the bottom row depicts the vertical (VL) and horizontal line (HL) surround stimuli respectively. The target element appeared in the missing space, either collinear with or orthogonal to the bar, at 3 degrees of eccentricity from the fixation cross on a 45 degree angle.

As the background surround stimulus remained stable for 18 trials before switching, it was important to prevent visual adaption to the stimulus, which could have reduced cortical responses (Maffei, Fiorentini, & Bisti, 1973). As there were inter-trial breaks between stimulus presentations, visual adaption would have occurred at a slower rate than the 30 seconds to 1 minute intervals reported (Blakemore, Muncey, & Ridley, 1973; Maffei, et al., 1973), where perception of the stimulus occurs for a disjointed 51

(18*1700ms/60) seconds. The next surround stimulus presented was rotated 90º so that new orientation-selective cells were being stimulated. Possible surround stimuli were selected randomly from a pre-generated list, which prevented two backgrounds with the same orientation being presented consecutively. Rotating the stimulus surrounds and targets in this way might also control for luminance artefacts due to the CRT monitor's raster scan that can alter horizontal and vertical grating perception (Garcia-Perez & Peli, 2001).

The 2AFC Task. Presenting stimuli on a trial-by-trial basis was important for improving the signal to noise ratio of the elicited waveform, and a 2AFC present/absent judgement was used to accomplish this. The task was included only to engage the subject, and correct or incorrect responses were not recorded (the subject was not aware of this). For this task, each time the target appeared, regardless of orientation or surround stimulus, there was a 50% chance of the target having a 1-pixel wide red line through the middle (Figure 18).

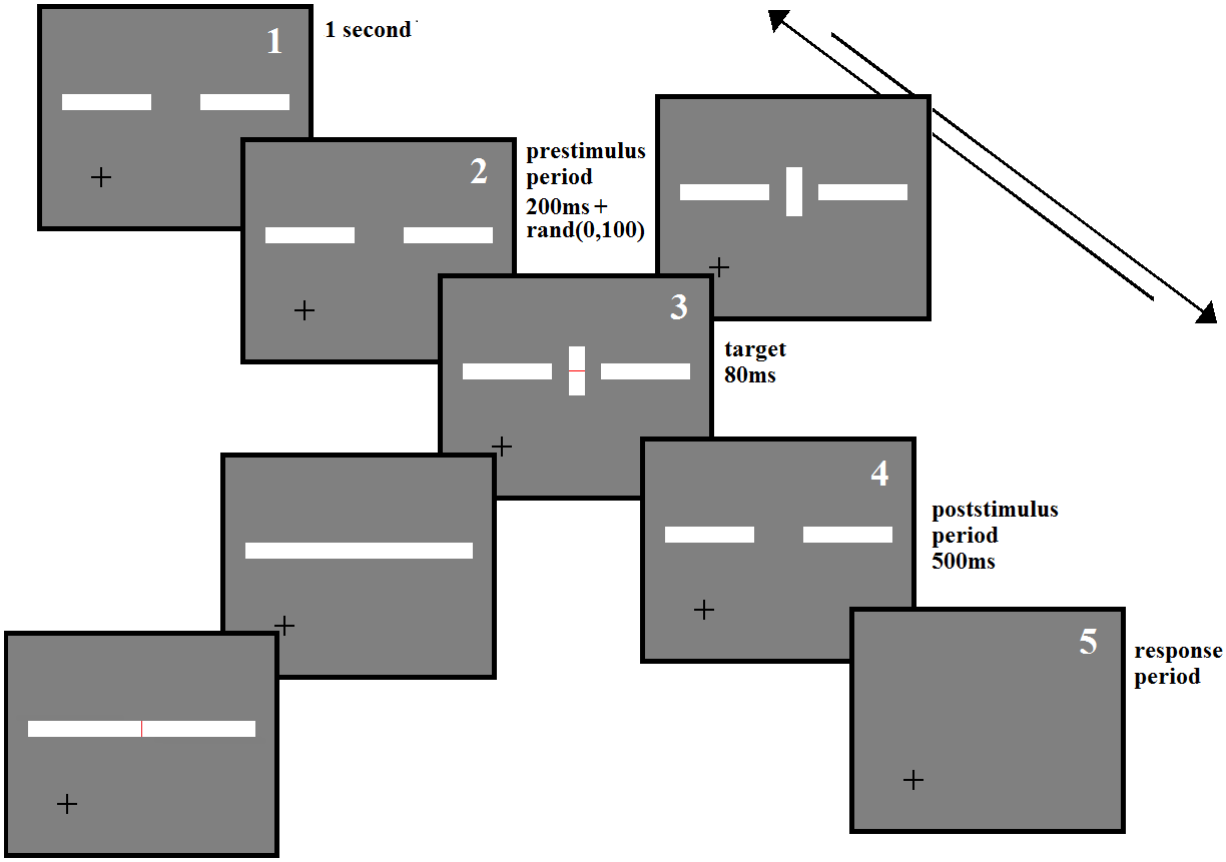

Figure 18. Trial progression on form completion paradigm. The surround stimulus displayed above is the horizontal line stimulus (HL), with an example of an orthogonal stimulus (3, top right) and collinear stimulus (3, bottom left), as well as an example of a target with a red stripe and blank for the 2AFC task (3). Each target displayed diagonally alongside (3) had a 25% chance of appearing. In the response period (5) there was white text at the bottom right prompting the participant to respond. After each response, the trial began again on the same surround stimulus, with a trial repeating 18 times followed by the surround stimulus changing to a rotated form.

At the end of each trial the subject was prompted to indicate whether the red line was present or not by pressing the ‘f’ or ‘j’ letter keyboard keys that had red (‘red line present’) and green tape (‘red line not present’) over them. The task was intentionally unrelated to the orientation to the visual stimulus as the goal was to increase attention

without directly interfering with perception of the target's alignment to the surround stimulus. This said, pilot testing suggested a task indicating the target's orientation (horizontal vs vertical) produced similar signal strength. During pilot experiments to develop the paradigm, runs were also tried in which there was no subject response, just passive viewing of the target pulsing on and off after an interstimulus interval (ISI). This allowed a faster rate of stimulus presentation, but did not seem to produce as strong a signal; hence it appeared that the use of a subject response created stronger engagement with the stimulus. The trials which included the red line were included in analysis, but are not thought to influence the waveform to the target due to the randomization of the appearance and due to the 2AFC task being unrelated to the main conditions being manipulated.

Generating Stimuli

The surround stimuli were manually drawn using an imaging editing program in such a way that the target appeared in the centre of the gap. The stimuli themselves were made of continuous thick white lines (Figure 17). The surround stimuli's location was adjusted so the target appeared directly in the gap with no horizontal or vertical misalignment.

Cortical Magnification Factor. The width of the target was originally scaled inversely to human cortical magnification factor to stimulate approximately equal areas on cortical area V1 on the basis of the target's retinotopic location (Schira, Wade, & Tyler, 2007). Given that the current method of retinotopic current analysis mapped the visual field for the range of eccentricities between one and twelve degrees (James, 2003), the target must appear within that range. Since form detection drops steeply in peripheral vision from 10 degrees of eccentricity (Hess & Dakin, 1997; Nugent, Keswani, Woods, & Peli, 2003) and this drop-off begins gradually from 1-2 degrees of eccentricity (Shani & Sagi, 2005), the target needed to be as close to the fovea as possible. Size parameters were

derived from Goh's (2008) retinotopic dartboard that suggested a width of 1.4 º of visual angle when the target is localized to 3 degrees of eccentricity on a 45 degree angle, at ring 14 (Figure 7). However, the width was approximately halved to 16 pixels, and the bar length extended to 45 pixels (Figure 16) to perceptually resemble a rectangle. The cortical area being stimulated is thus only roughly scaled to cortical magnification factor. The top right visual field quartile was used (see Figure 17).

Localizing the target within a contour at 3 degrees of eccentricity has been demonstrated to evoke form perception-related waveforms, so this can be considered an appropriate location (Mathes, et al., 2006). The target was located in the same position for every surround stimulus, including rotated ones. In addition, the rotated surround stimuli extended to similar distances within the periphery, so a bias due to peripheral presentation is not expected between stimulus orientations (see Table 1).

Table 1

Stimulus Extensions in the Visual Field by Degree of Visual Angle

	VL	HL	VS	HS
Up	5	2.2	5	2.3
Down	1	-	1	3.7
Left	-	1	3.7	1
Right	2.2	5	2.3	5

Note. These measurements were made from the fixation cross in the centre of the screen to the outermost point of the stimulus. Each side was 6cm long or 6 degrees of visual angle in length.

Data Processing

Recording was conducted in a darkened audio-proof room with Faraday shielding. The BioSemi system has the first-stage of amplification integrated with the electrodes. This makes the signal essentially immune to electromagnetic interference,

irrespective of the scalp impedance. Data was baseline corrected using a median filter with a 2 second moving window; that is, for each channel, a baseline signal taken as the running median in a two second window is calculated, and that baseline is subtracted pointwise from the recorded data. This removes the large offset and drift values which are characteristic of the BioSemi recordings. The data was also average referenced, by subtracting at each time-point the average across all channels. Signals were later low-pass filtered with a third-order Butterworth filter, with cutoff frequency 40Hz, in forward and backward direction to produce zero phase distortion. Outliers in the data such as electrode malfunctions and eye blinks were removed with an algorithm that detected points if they had magnitude more than ten times the median absolute value for that channel, and excluded those points within 0.11 seconds before and after (to avoid having unusable short segments remaining). As most eye blinks occurred during the inter-trial breaks, no trials had to be removed as a result of missing data.

For each run, the evoked responses for each channel and stimulus condition are fitted as linear combinations of empirically-derived basis waveforms over the time-window 0 to 0.6 seconds relative to stimulus onset, with a tenth-order autoregressive model for the noise signal (Goh, 2008). This is equivalent to the calculation of a stimulus-triggered average but produces a cleaner signal in that the empirical basis waveforms driven by the stronger signals provide an enhanced estimation of amplitude in the channels where signal is weaker. It also implements an error model which better matches the low-frequency biological noise in the signals.

Results

Topographic Data Reduction

Use of a spatial principal components analysis (PCA) can allow the extraction of statistically defined components of waveform topography which can dramatically reduce the dimensionality of data and provide a summarised description of electrical field

topography (Skrandies, 1989). In this case a Singular Value Decomposition (SVD) was used, which decomposes the two dimensional data array of channel vs time/condition/subject/repeat into a mean value per channel, plus linear combinations of channel profiles, of decreasing order of contribution to the signal power. It is equivalent to a PCA applied to the covariance matrix between channels (Gerbrands, 1981).Three factors were extracted from the first 300ms of data. All factors were internally consistent and well defined by the variables; the lowest of the squared multiple correlations was .70, all three accounting for over 90% of the variance (Figures 19, 20, and 21).

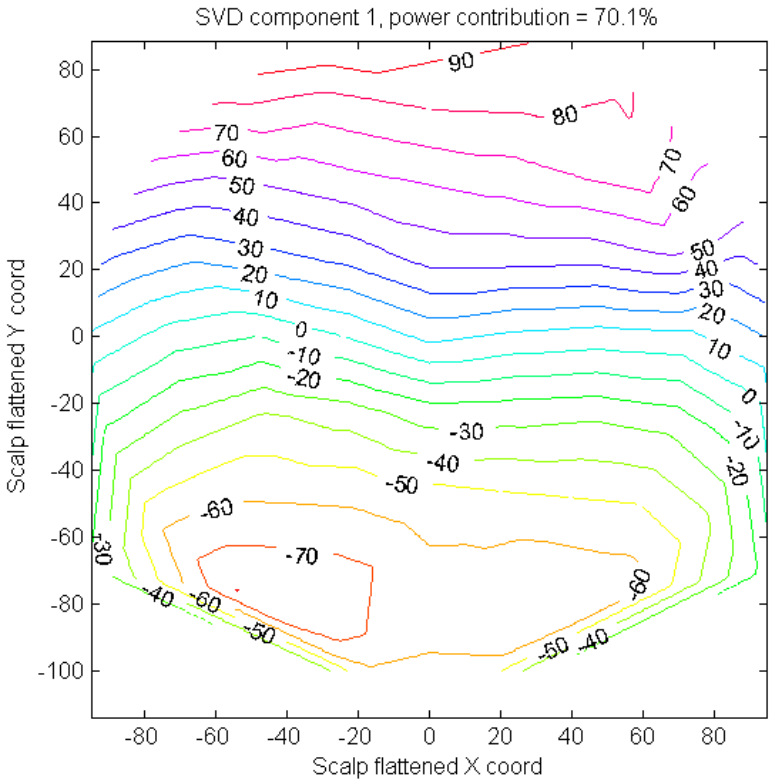

Figure 19. SVD component 1. Normally the X and Y values would be represented in a 3D space to account for the electrode coordinates but for the sake of visualization have been transformed for representation in a 2D space. The largest component loading value is at the frontal red line (90µV). Each field line corresponds to a drop of 10µV. The extreme negative value is -70µV, located over the left occipital lobe, as is expected for a target in right visual field.

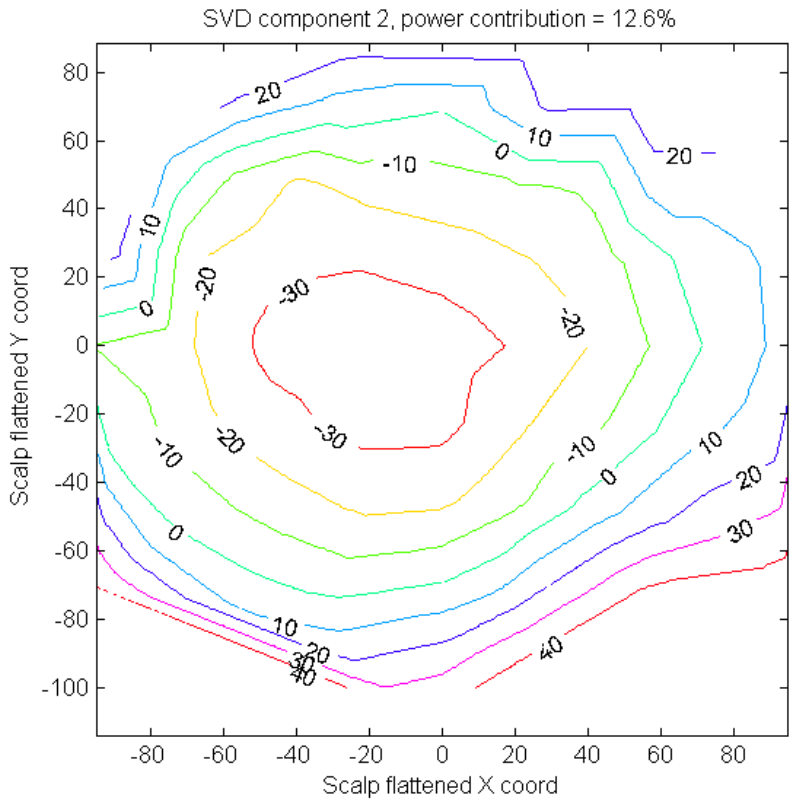

Figure 20. SVD component 2. Normally the X and Y values would be represented in a 3D space to account for the electrode coordinates but for the sake of visualization have been transformed for representation in a 2D space. The largest component loading value is at the occipital red line (40µV). Each field line corresponds to a drop in 10µV. The extreme negative value is -30µV, localized in a central-parietal position.

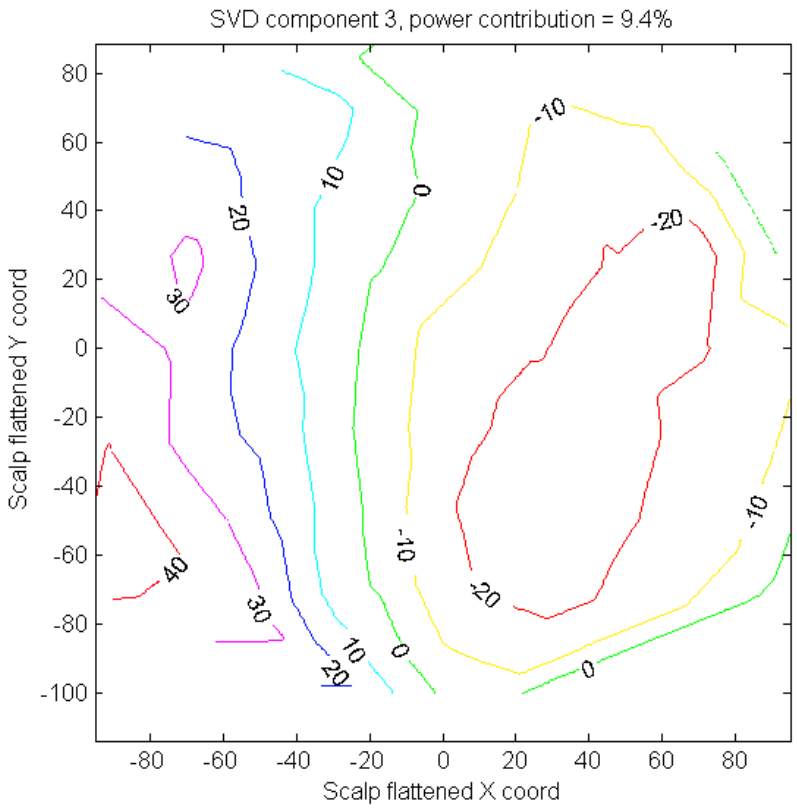

Figure 21. SVD component 3. Normally the X and Y values would be represented in a 3D space to account for the electrode coordinates but for the sake of visualization have been transformed for representation in a 2D space. The largest component loading value is at the occipital red line (40µV). Each field line corresponds to a drop in 10 µV. The extreme negative value is -20µV, localized in a lateral position.

Waveform Analysis

The waveform data-frame was made in MATLAB version 2014a (MATLAB; The Mathworks, Natick, MA) and exported to R version 3.0.1 for analysis (Team, 2014). The analysis used custom code written by Dr. Andrew James and R packages lme4 (Bates, M, Bolker, & S, 2014), lattice (Sarkar, 2008), Matrix (Bates & Maechler, 2014), reshape (Wickham, 2007), Rcpp (Eddelbuettel & Francois, 2011) and R.matlab (Bengtsson, 2014).

Stimulus presentation elicited a stereotypical waveform with characteristic positive and negative peaks (Figure 22, above). The between-subject variability was large (Figure 22, below, and Figure 23).

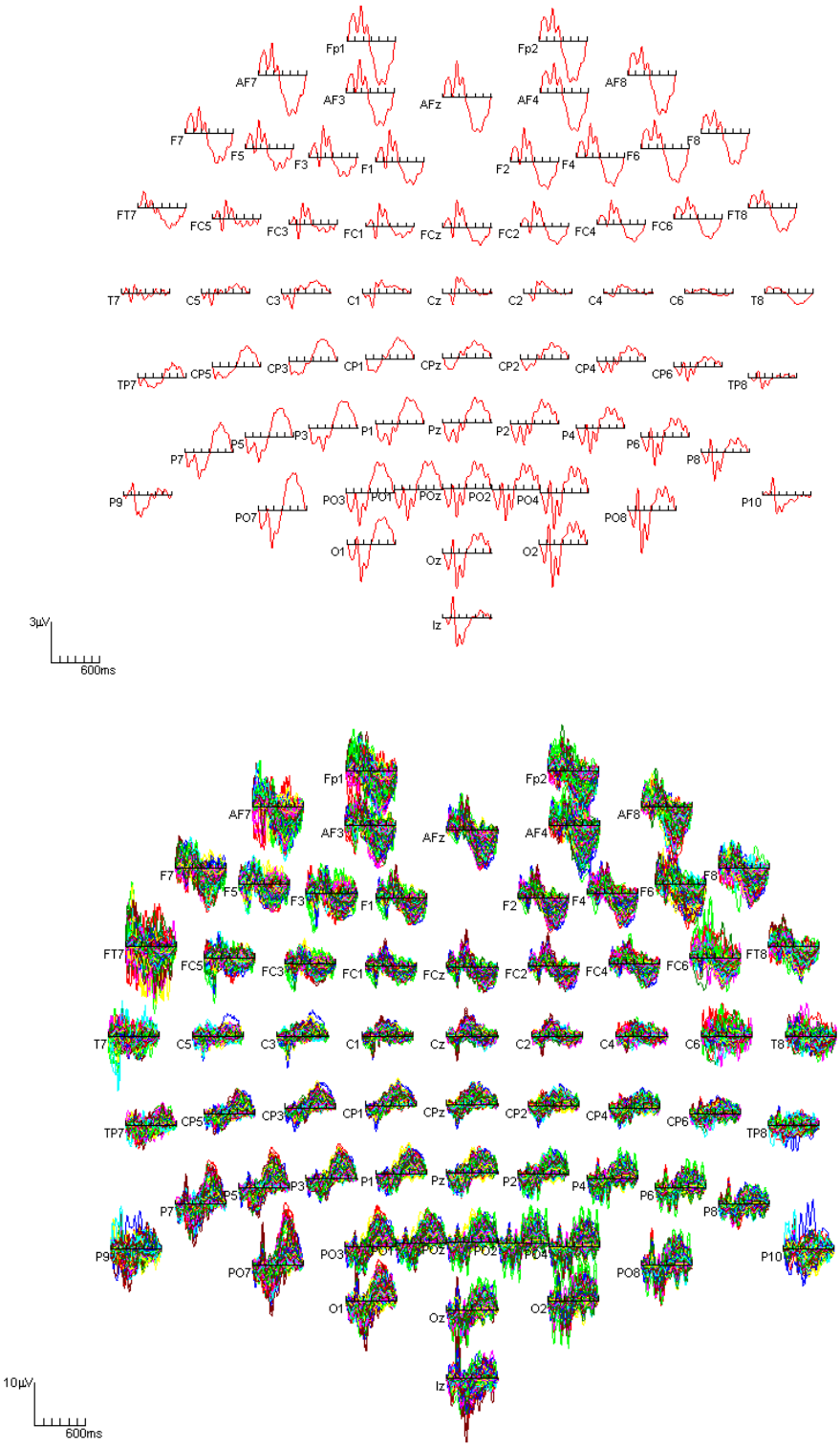

Figure 22. Waveform scalp plots. Above: The mean elicited waveform taken over all conditions, subjects, and repeats. Below: Between-subject waveform variation over all conditions and repeats. Each coloured line corresponds to a subject.

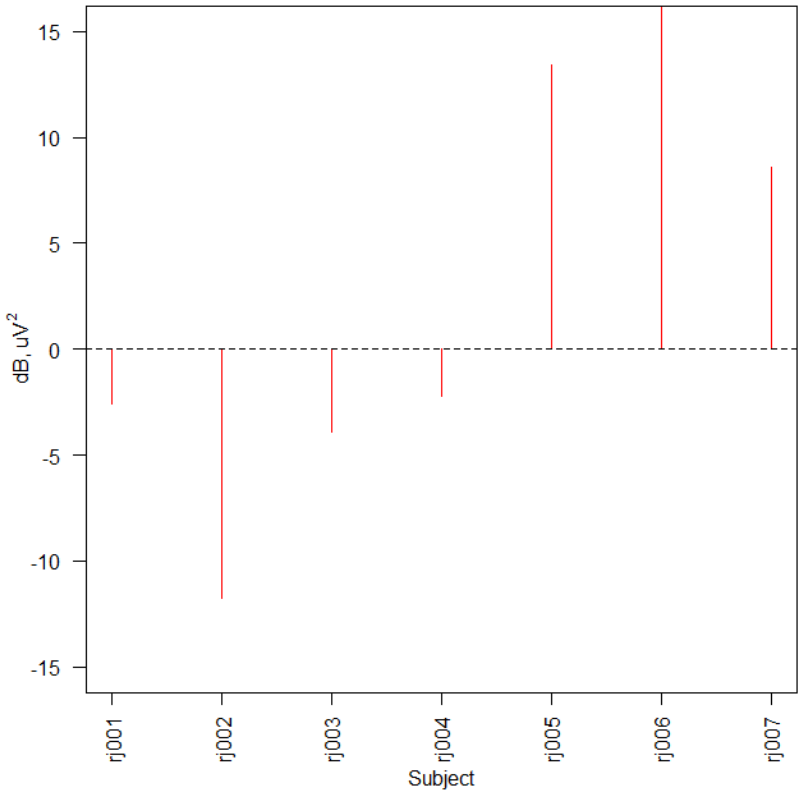

Figure 23. Subject median waveform amplitude. Decibels (dB), or the logarithmic ratio is relative to rj004 set to 0 and allows the inference of magnitude difference of amplitude. -2.24 is the subject error subtracted from all subject dB values. The subject error is each subject's median amplitude minus the median amplitude of all aggregated subjects. Subject rj002 has the smallest amplitude and subject rj006 has the largest.

As there is such diversity in subject cortical folding including the size of areas V1 and V2 (Amunts, et al., 2000), aggregating subject waveforms using a mean statistic to examine between-condition differences was considered inappropriate as it might lead to signal cancelling or distortion due to this variation alone.

An alternative method of aggregating subject data over channels uses global field power (GFP) or the global field root mean square (GFRMS) (Lehmann & Skrandies, 1980; Skrandies, 1989, 1990) which aggregates all scalp electrodes together and

measures the square-root of mean signal power over channels, and hence summarizes the amount of activity at each time point:

$$RMS(v) = \sqrt{\frac{1}{n}\sum_{i=1}^{n} v_{i^2}} \quad (1)$$

where n is the number of electrodes (64 in the case of the full-head power, or a subset of eight of the most occipital channels, as defined below) and v is the vector of signal values across channels at a time point, in microvolts. GFP can be plotted over time in milliseconds, and allows the periods of activity to be examined. Note the signals are already average-referenced, so that the mean value is zero at each time point when all 64 channels are considered, but for the subset of eight channels, the signals are relative to the whole-head mean potential.

Reducing the number of temporal data points to compare is of interest to make data analysis more manageable. Given minor latency variations in peaks between subjects (Figure 24) and on the basis of the prior literature review, the mean values of 3 time windows were examined: 100-150ms, 150-200ms, and 300-350ms.

Linear Modelling

Three additive linear models were tested in R version 3.0.1. First the response activity over the eight most occipital channels were pooled (‘POz', 'Oz', 'Iz', 'Pz', 'PO1', 'PO2', 'O1', and 'O2’) by calculating the RMS as above to produce the dependent variables. There is a significant subject-wise variation in scale of evoked potentials due to differing resistance properties of the skull, and hence data was corrected by a scale-factor for each subject to bring the overall RMS for each subject to the middle value over the seven subjects. Subject was later fitted as an additive factor to the log-transformed signal strength, however the correction in scale at this stage facilitates comparative plots of the signals across subjects.

Three values were then extracted from each GFRMS waveform, as measures of activity over three time windows, 100-150ms, 150-200ms, and 300-350ms. These time windows covered peaks of activity, as seen in Figure 24, the boundaries marked as vertical dashed lines.

The three response measures were transferred to the R package for linear modelling, along with factor levels for subject (7 levels), orientation of the surround stimulus (2 levels), stimulus collinearity (2 levels), surround type (2 levels), and repeat (2 levels). This gave a total of 7*2 *2*2*2=112 mean data points for each of the three time-window measures. Linear models were fitted with a log-transform of the response strength, calculated by taking the decibel power, that is:

$$dB = 10*\log_{10}(GFRMS^2) = 20* \log_{10}(GFRMS) \quad (2)$$

Note that the value $10*\log_{10}()$ of the global field power in μV^2, is equal to $20*\log_{10}()$ of the global field RMS, GFRMS, in μV, by properties of the logarithm function (Table 2).

Table 2

Linear Models of Waveform Differences by Time Window

Time Window		**Coefficients**	**Estimate Std. Error**	**t value**	**p <**
100-150ms	**Adjusted R^2=0.204**				
	Intercept(rj001)	4.949	1.148	4.313	0.001
	rj002	-5.597	1.295	-4.323	0.001
	rj003	-1.467	1.295	-1.133	*ns*
	rj004	-2.073	1.295	-1.602	0.001
	rj005	-5.188	1.295	-4.007	0.01
	rj006	-4.038	1.295	-3.119	0.01
	rj007	-3.858	1.295	-2.980	*ns*
	Collinearity	0.778	0.692	1.124	*ns*
	Surround Orientation	0.479	0.692	0.693	*ns*
	Surround Type	0.394	0.692	0.569	*ns*
	Repeat	-1.718	0.692	-2.482	0.05
150-200ms	**Adjusted R^2 =0.517**				
	Intercept(rj001)	9.089	1.030	8.825	0.001
	rj002	-6.650	1.162	-5.723	0.001
	rj003	-0.614	1.162	-0.529	*ns*
	rj004	-5.802	1.162	-4.994	0.001
	rj005	-9.462	1.162	-8.144	0.001
	rj006	-2.482	1.162	-2.136	0.05
	rj007	0.090	1.162	0.077	*ns*
	Collinearity	-0.122	0.621	-0.196	*ns*
	Surround Orientation	-0.419	0.621	-0.674	*ns*
	Surround Type	-0.002	0.621	-0.003	*ns*
	Repeat	-0.921	0.621	-1.483	*ns*
300-350ms	**Adjusted R^2 =0.466**				
	Intercept(rj001)	1.141	1.070	1.066	*ns*
	rj002	-6.039	1.207	-5.002	0.001
	rj003	0.691	1.207	0.573	*ns*
	rj004	2.994	1.207	2.480	0.05
	rj005	3.857	1.207	3.195	0.01
	rj006	-2.716	1.207	-2.249	0.05
	rj007	-3.015	1.207	-2.497	0.05
	Collinearity	0.203	0.645	0.315	*ns*
	Surround Orientation	-0.314	0.645	-0.487	*ns*
	Surround Type	0.869	0.645	1.346	*ns*
	Repeat	-0.994	0.645	-1.540	*ns*

Note. Tables of results from R package have columns showing regression coefficient, standard error, T-statistic, and p-value for a two sided test against H_0: $\beta=0$, and rows corresponding to components as marked: the first row giving the intercept, being the

global field power (dB) for the case when each factor is at its first level, with subsequent rows being incremental contrasts relative to that case. Values are rounded to 3 decimal places.

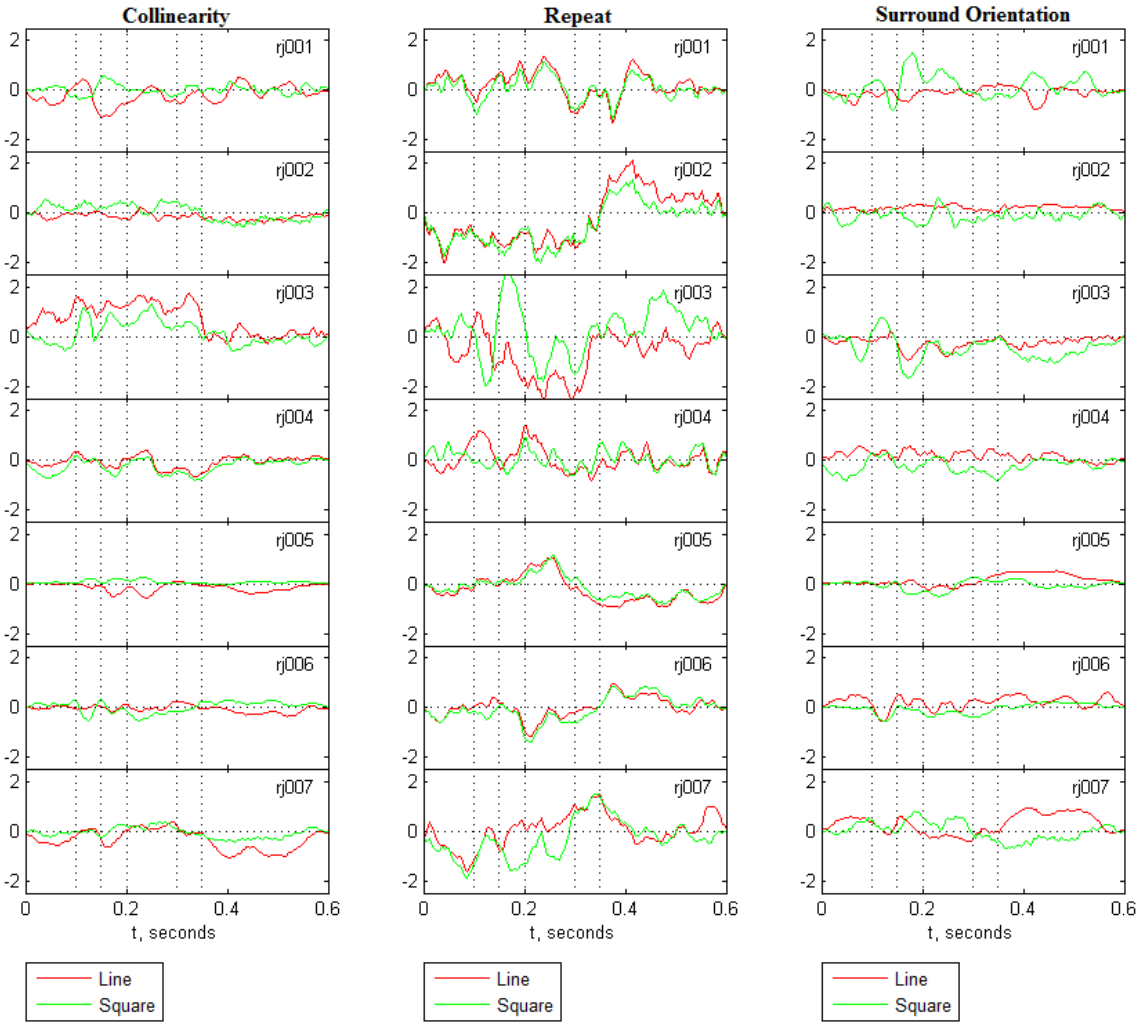

Figure 24. Line and square surround difference waveforms. Each column represents the difference waveforms for the square and line surround for collinearity, repeat, and surround orientation respectively. The five dotted vertical lines mark the three time-windows from which a mean was obtained: 100-150ms, 150-200ms and 300-350ms. The Y axis displays the subject-corrected difference waveforms in μV. These windows appropriately capture the peaks at each of these time points.

Each of the three linear models were statistically significant with small to moderate adjusted R^2 values (Table 2). Significant effects were observed in the 100-150ms time window for subject and repeat only. Significant effects were observed in the 150-200ms and 300-350ms time window for subject only. Collinearity and surround type were non-significant at each time window. This result supports the null hypothesis and suggests the study manipulation of surround type and collinearity level was too subtle to detect or did not work. Examining differences at the V1 and V2 level for subjects rj001 and rj002, the subjects with MRI/fMRI cortical maps, may allow feedback to be inferred at a given time-period on the basis of stimulus condition.

Source Analysis

Several steps are required before a source estimate can be reached for the waveforms obtained in this study.

First, the responses obtained from the fMRI multifocal analysis are decomposed to separate compound responses to components attributable to each stimulus region (Vanni, et al., 2005). Then they are then further analysed with multiple linear regression to provide an optimal estimate of each component (James, 2003).

Second, a head model is then required to describe electrical conductivities in V1 and V2 including signal cancelation, inter-subject variability (Ahlfors, Han, Belliveau, et al., 2010; Amunts, et al., 2000; James, 2003), and dimensions of the head given the obtained MRI (note: not fMRI) cortical maps. The three-sphere Berg model was used (Berg & Scherg, 1994) to segment the ‘three spheres’ comprising the outer boundary of the brain, the skull, and the scalp. Scalp tissue is assumed to have the same conductivity as the brain (Berg & Scherg, 1994) (Figure 25), with the skull being a higher-resistance barrier in between.

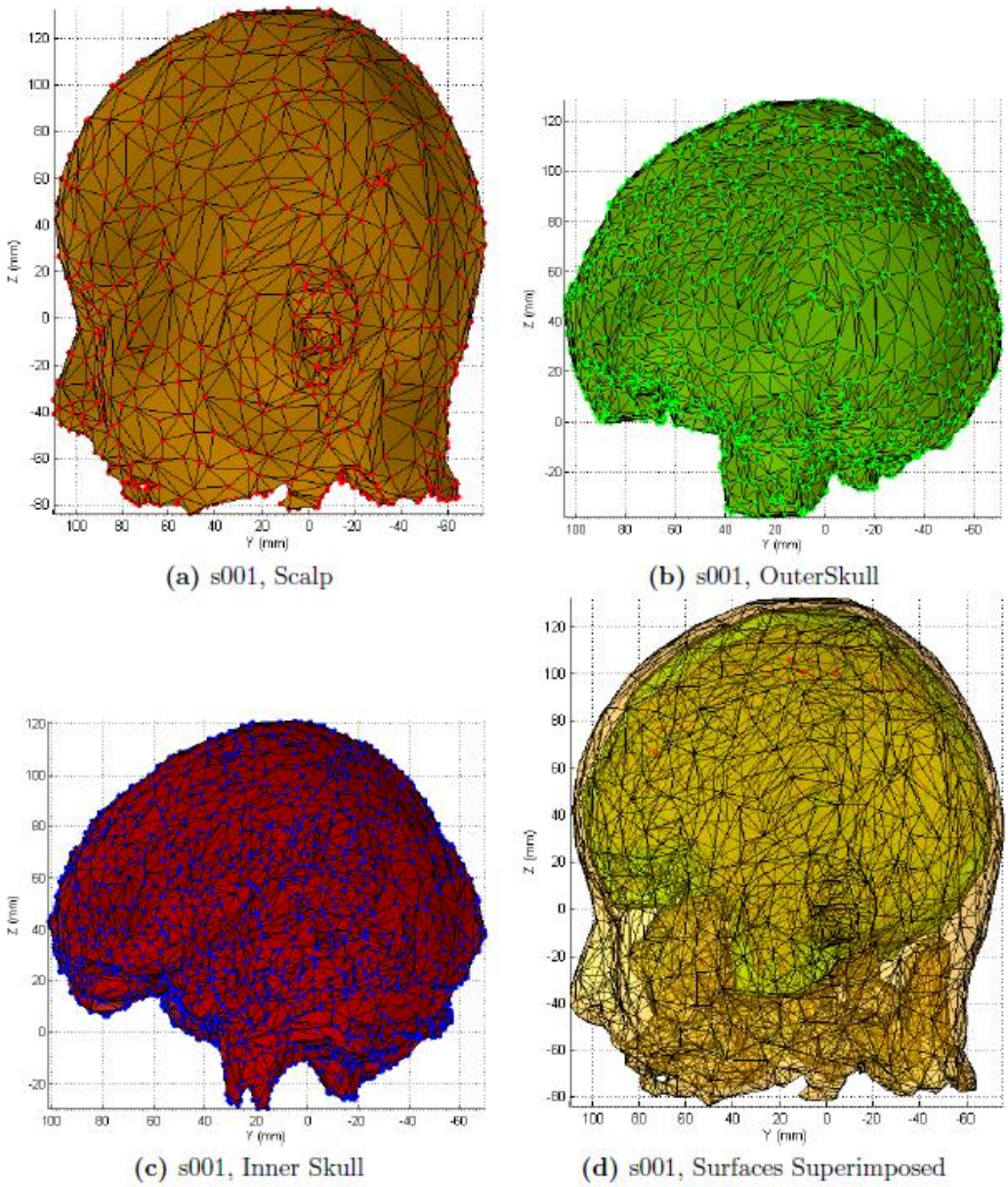

Figure 25. Three sphere head model for subject s001. The segmentation of the scalp, outer, and inner skull using the three-sphere Berg model is observed for subject s001. Subject s001 is the same subject as rj001 in the current study, reflective only of code name differences. Adapted from Goh (2008).[7]

The third step involves computing the inverse solution by combining the fMRI and MRI models. The Boundary Element Model (BEM) of source analysis can contribute to this forward model by triangulating or panelling surfaces from the MRI

image (Pruis, Gilding, & Peters, 1993) and mapping the multifocal data to this (Figures 26 and 27).

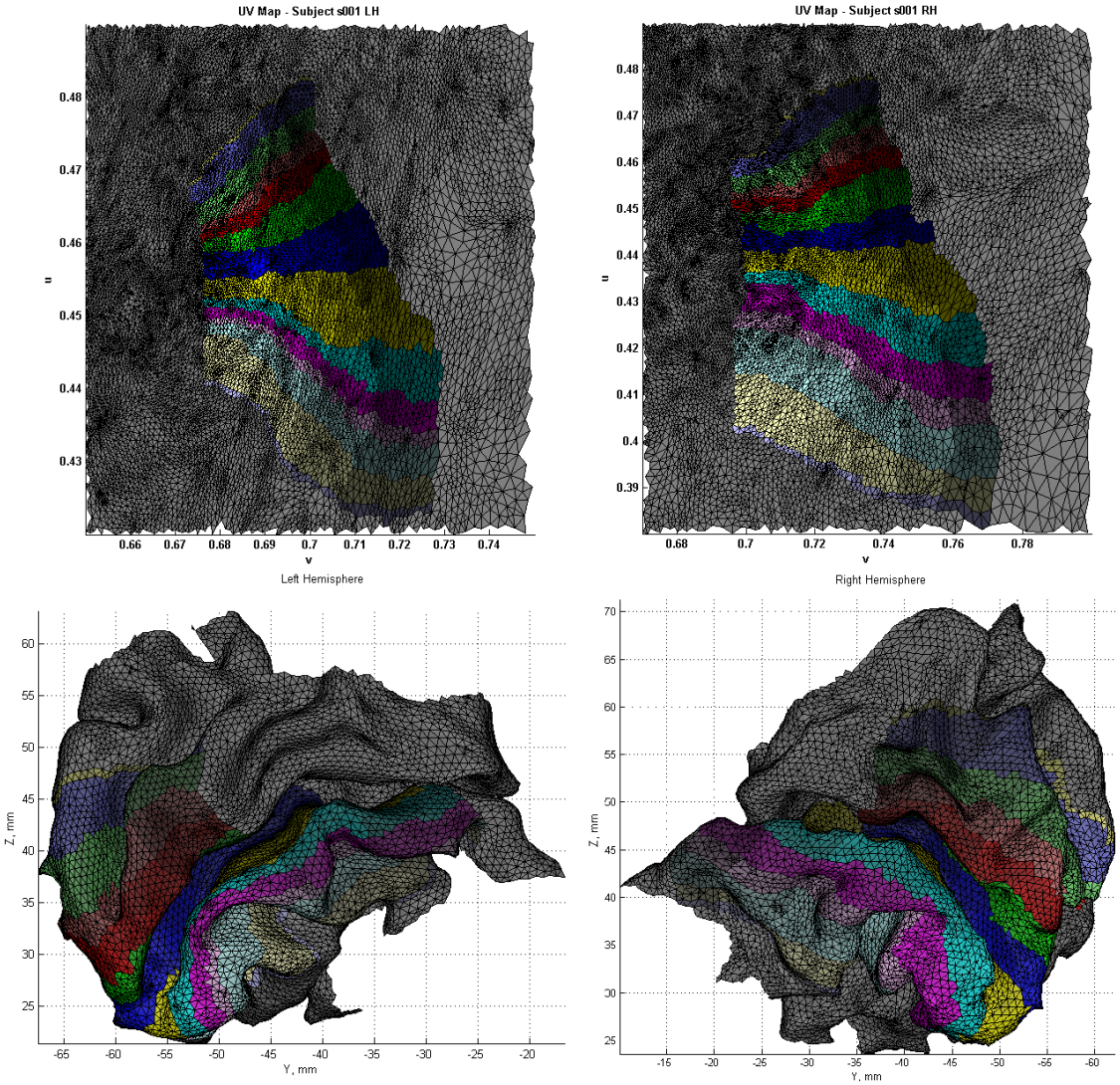

Figure 26. Participant s001's visual field fMRI/MRI map. The top images shows the visual field map and the bottom images show the maps as projected onto the folded cortex for the left and right hemispheres, respectively. Subject s001 is equivalent to rj001 in the current study. Adapted from Goh (2008).[7]

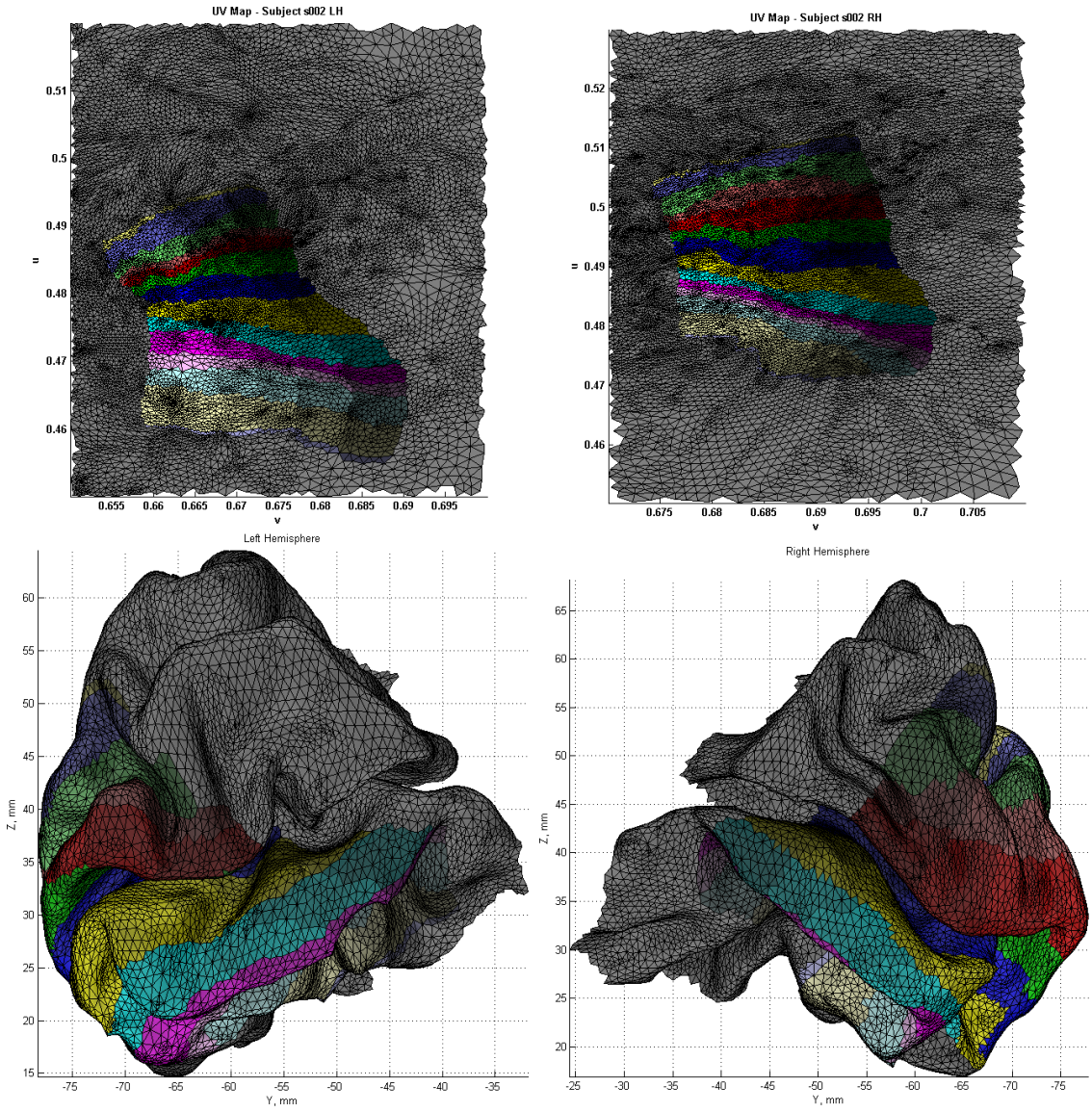

Figure 27. Participant s002's visual field fMRI/MRI map. The top images shows the visual field map and the bottom images show the maps as projected onto the folded cortex for the left and right hemispheres, respectively. Subject s002 is equivalent to rj002 in the current study. Adapted from Goh (2008).[7]

Finding the inverse solution involves adding source dipole orientations to the MRI model based on cortical folding which can lead to more accurate EEG dipole estimates (Ahlfors, Han, Belliveau, et al., 2010) (Figures 28, 29, and 30).

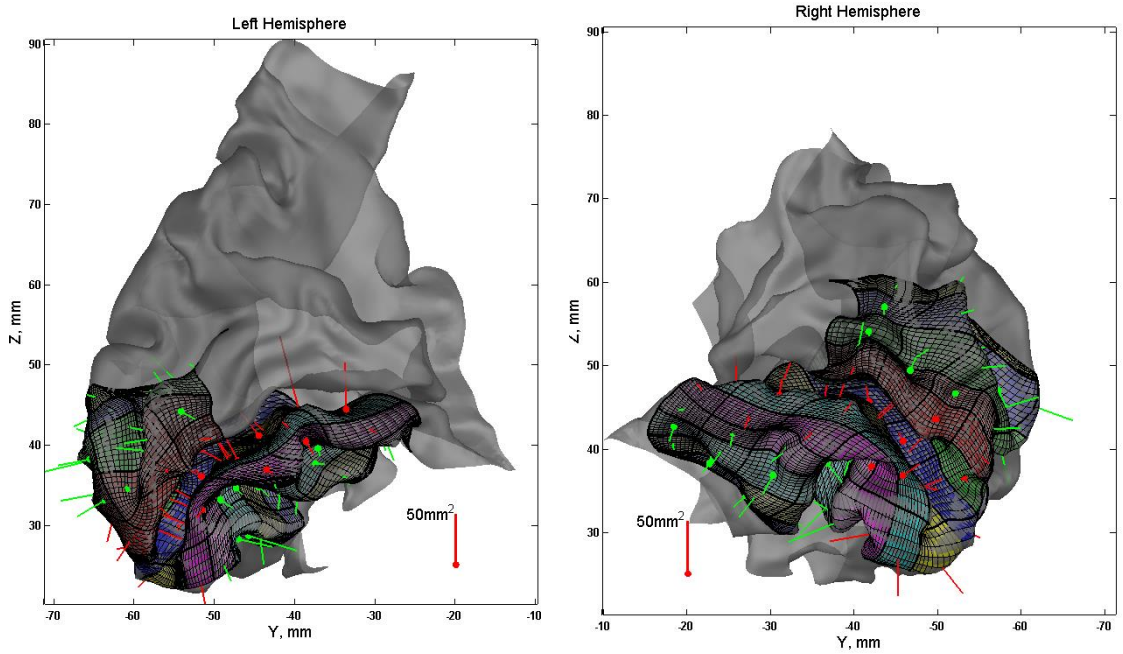

Figure 28. Subject s001's dipole map. Fitted dipoles using the 3-sphere Berg model. V1 vectors are in red and V2 vectors are in green. Subject s001 is equivalent to rj001 in the current study. Adapted from Goh (2008).[7]

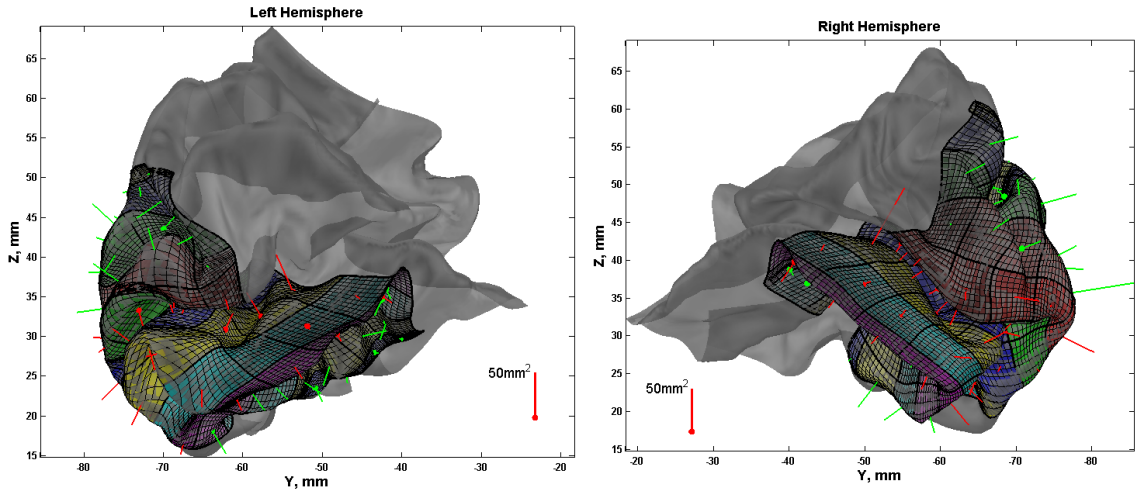

Figure 29. Subject s002's dipole map. Fitted dipoles using the 3-sphere Berg model. V1 vectors are in red and V2 vectors are in green. Subject s002 is equivalent to rj002 in the current study. Adapted from Goh (2008).[7]

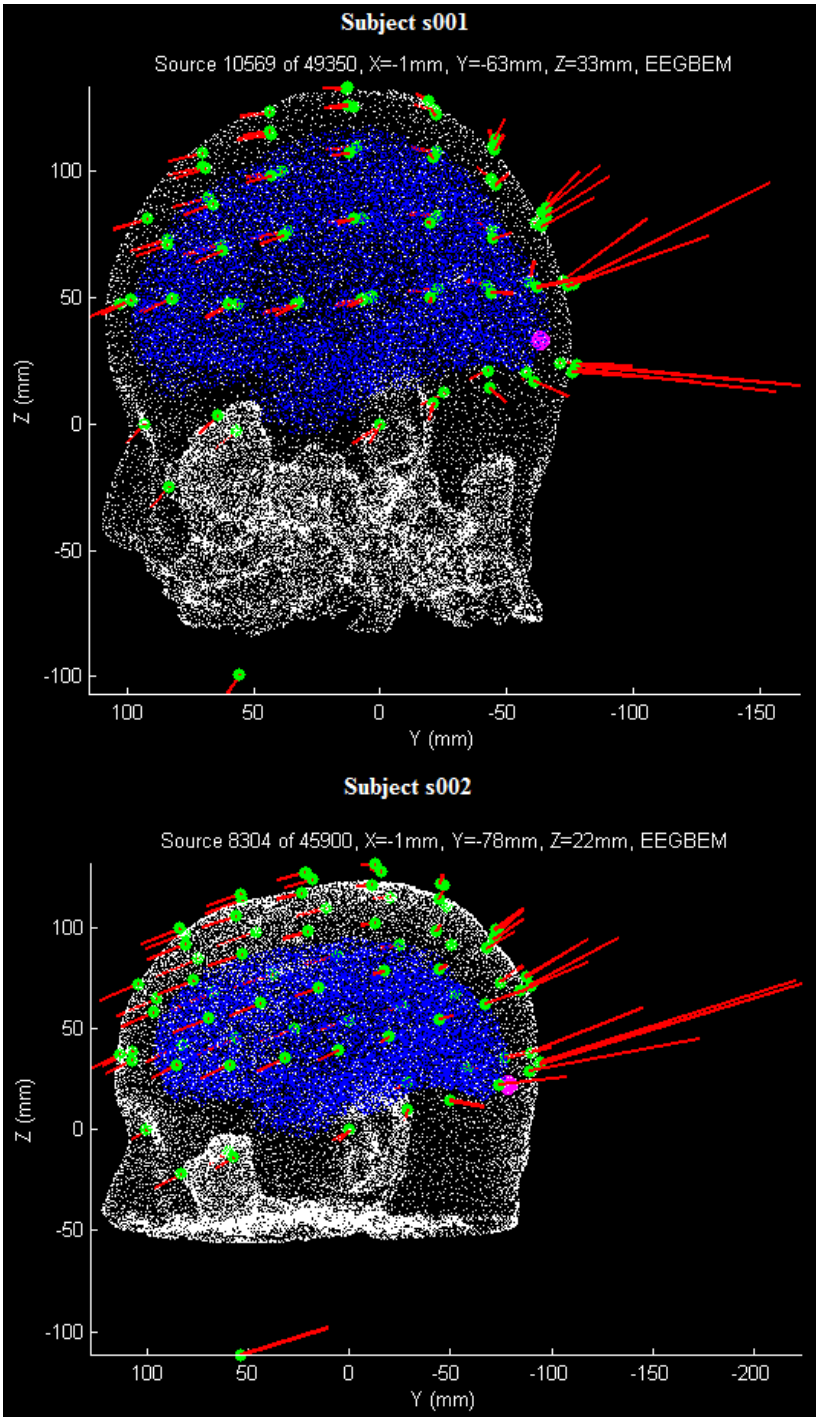

Figure 30. Forward model for s001 and s002. For a dipole marked in magenta the red vectors plotted at each electrode location give the direction and length (relative coupling coefficient from dipole strength) of the dipole that would be most effective, in nAm to potential. Predicted potentials are the dual-pairing of the dipole vector at the source, with gain co-vector for each electrode. Subjects s001 and s002 are equivalent to rj001 and rj002. Adapted from Goh (2008).[7]

The length of the dipoles, defined by a vector with a mean orthogonal direction to the cortical region (N (x, y, z) mm^2), represents the effective dipole strength including any cancellations due to cortical folding. The strength is measured by the current times dipole length in units of *nAm*. This is equivalent to *μAmm* and allows the interpretation of signal strength in terms of cortical current. This allows for the inference of feedback based on the direction and strength of the currents within the V1 and V2 cortical sheets.

Subjects rj001 and rj002 had their EEG waveforms decomposed into V1 and V2 cortical currents using custom code in MATLAB (version 2014a), written by Dr Andrew James. For each subject, the forward model produces a matrix of gains, from the V1 and V2 patches, to the 64 EEG channels. This matrix functions as a 64x2 sized design matrix, which predicts the set of 64 potentials at any time for the two values of current dipole density within the V1 and V2 patches of cortex which map the visual field location in which the target is pulsed. Solving the inverse problem at each time point is then the minor calculation of regressing the 64 EEG potential values on the forward model design matrix, to estimate the two current dipole densities. The estimation can be made more efficient by using a weight matrix which reflects the covariance between the 64 channels. It was found however that more stable estimates were produced by a more conservative method, which weighted inversely by the estimated variance in each channel, but did not use correlations between channels. Note that the choice of weight matrix does not bias the estimates, and the full expression involving the channel covariance matrix is still used for estimating the variance and standard errors of the current dipole densities.

The R-squared values for the fit of evoked potential in terms of source current had mean values over time/condition/repeat equal to 0.62 for subject rj001 and 0.42 for subject rj002, indicating the proportion of signal power fitted by the source analysis.

The angles between the V1 and V2 dipoles for the visual field location of the target were 140^{o} for rj001, and 49^{o} for rj002. Although orthogonal dipoles would have been the optimum, these angles are still far from collinear, and hence the currents are not confounded and can be separated by regressing on the forward model gain matrix, as above.

The source current signals were organised by condition to allow for statistical significance in V1 and V2 to be tested (Figures 31 and 33) and hopefully offer insight into the non-significant linear model analysis of global field power for stimulus surround and collinearity. Statistical differences between the orthogonal target and collinear target for the line and square surround stimulus were tested within V1 and V2 for subjects rj001 and rj002 using a two-sided test running t-statistic corresponding to a significant difference calculated at each time point in the waveforms. Note that this form of presentation does not constitute a formal test of significance as it represents multiple tests without correction for multiple comparisons, but is given as a graphical representation of where in the waveforms there may be significant effects of the manipulation of stimulus conditions (Figures 32 and 34).

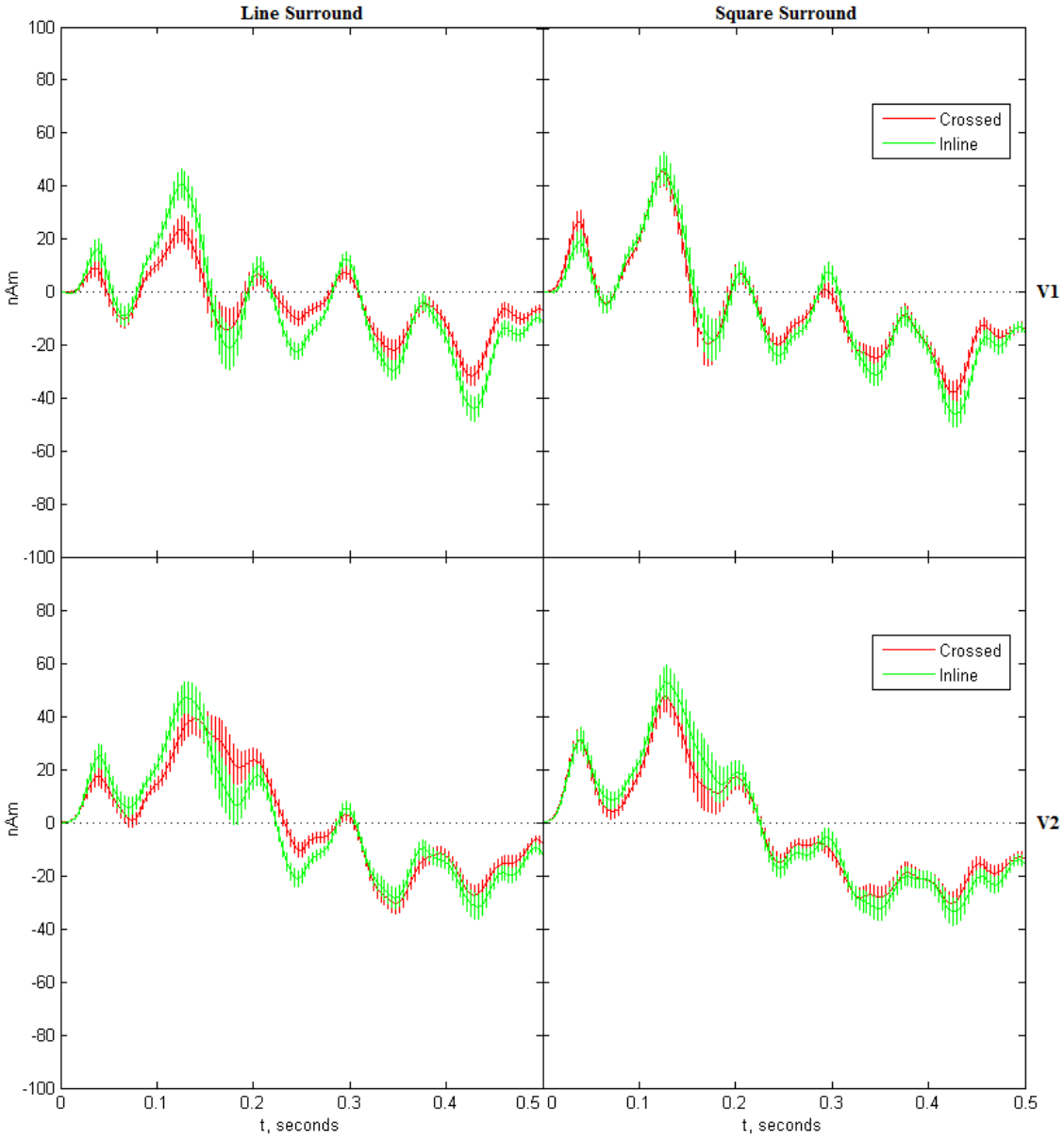

Figure 31. Subject rj001 source signals. Error bars represent +/-1 SE from the estimate. The top row includes the V1 currents and the bottom row the V2 currents. ‘Crossed’ refers to the target when it is orthogonal to the surround stimuli, and ‘Inline’ refers to when they are collinear to the surround.

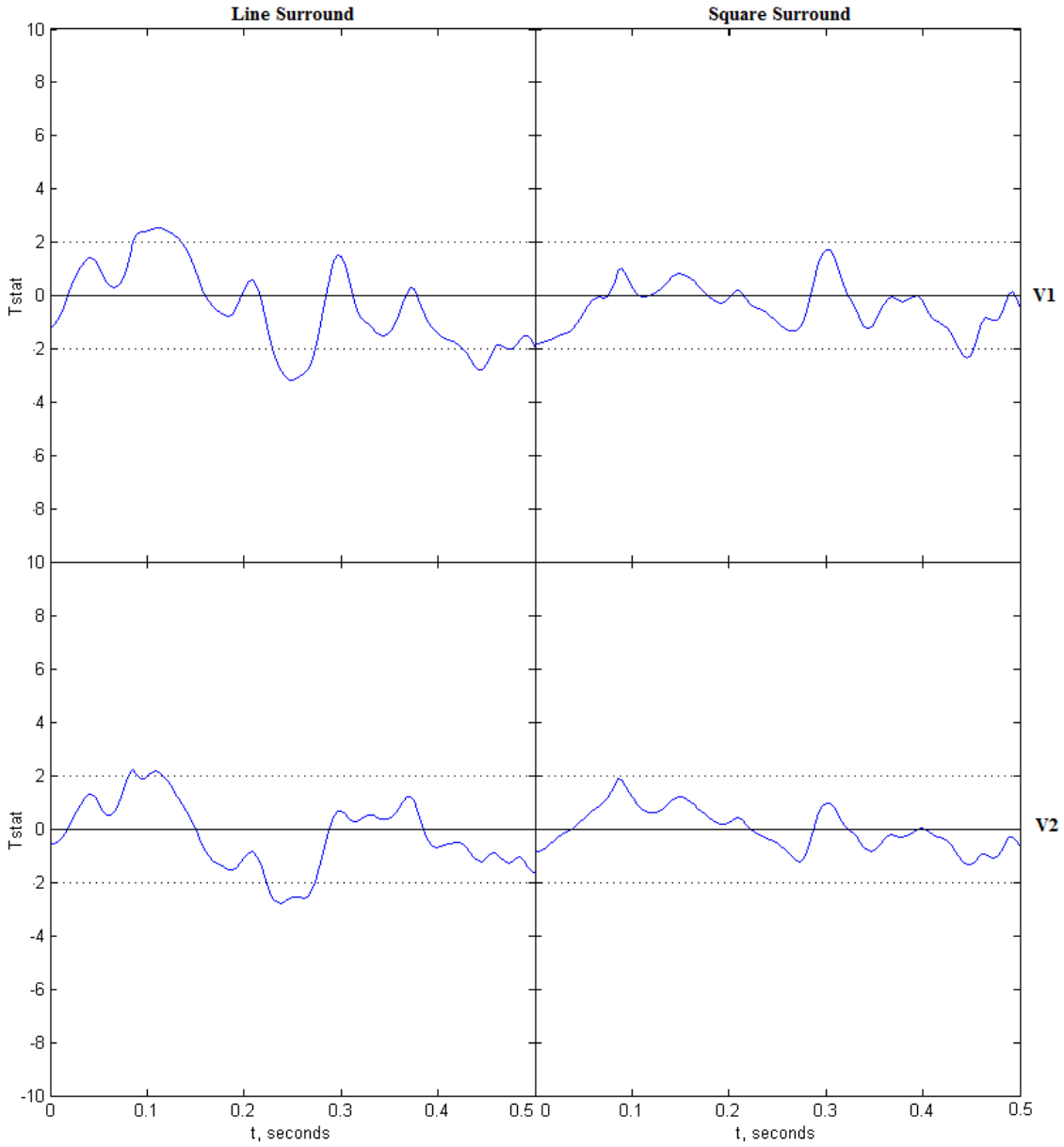

Figure 32. Subject rj001 running t-test on source signals. A T-stat of 2 (dotted line) represents a significance level of $p = 0.05$ for a two-sided test.

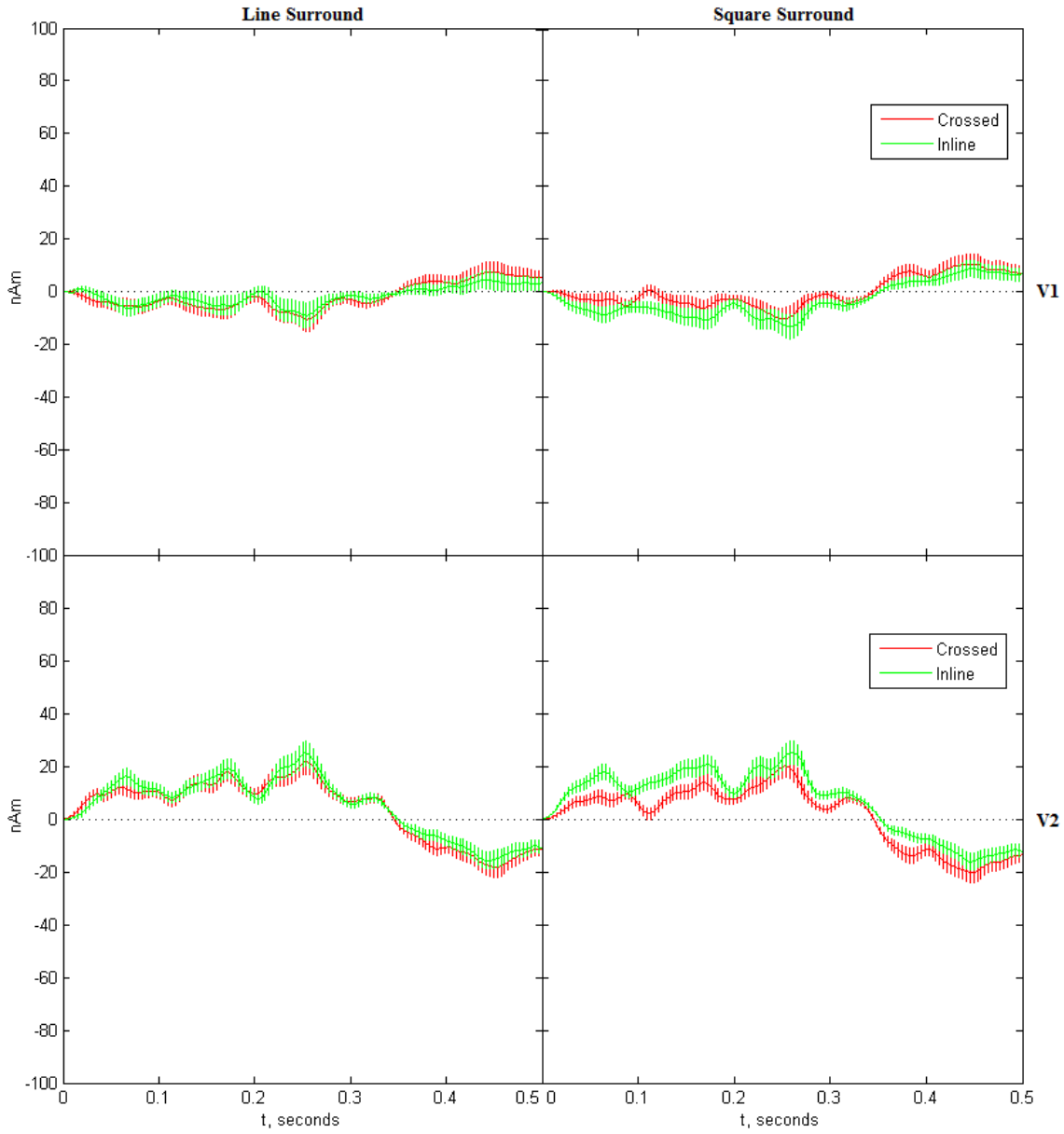

Figure 33. Subject rj002 source signals. Error bars represent +/- 1 SE from the estimate. The top row includes the V1 currents and the bottom row the V2 currents. ‘Crossed’ refers to the target when it is orthogonal to the surround stimuli, and ‘Inline’ refers to when they are collinear to the surround.

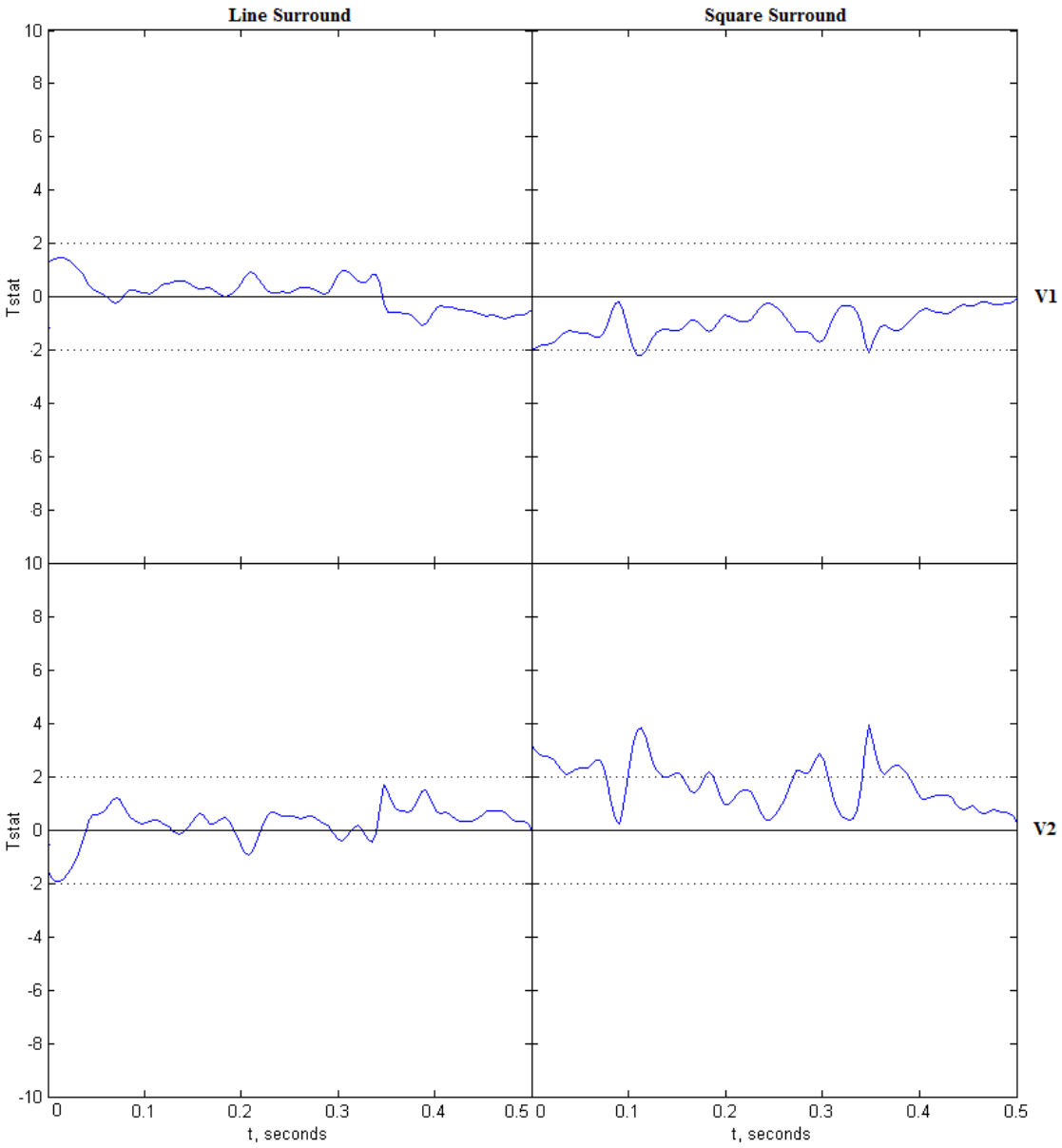

Figure 34. Subject rj002 running t-test on source signals. A T-stat of 2 (dotted line) represents a significance level of $p = 0.05$ for a two-sided test.

The running t-test (abs(T)> 1.96, p <.05, df = 63, >40,000) revealed inconsistent differences in V1 and V2, by subject, and by condition (for ease of reference, see Table 3 for significant time regions).

Table 3

Summary of Main Current Effects by Stimulus Collinearity

Subject	Brain Region	Surround Stimulus	Time Values of Peaks with p <.05
rj001	V1	Line	100ms, 250ms, 450ms
		Square	450ms
	V2	Line	100ms, 250ms
		Square	-
rj002	V1	Line	-
		Square	100ms, 350ms
	V2	Line	-
		Square	100ms, 300ms, 350ms

Note. The time values of the peaks are rough estimates.

Regarding the cortical currents in V1 and V2, several time periods seem to be associated with differences in the direction of the currents, particularly for subject rj002 where V1 and V2 reflect opposing current directions (Table 3 and Figures 33 and 34).

Specifically, around 100ms for subject rj002 the square surround stimulus produces statistically significant differences between collinear and aligned stimuli relative to the line surround and this is true in V1 and V2. The V1 current is negative and the current in V2 is positive indicating potential interacting currents in the cortical sheets.

Alternatively, for subject rj001 there were positive going currents in V1 *and* V2 for the line surround a negative going current in both regions around 250ms. That V1 and V2 have currents going in the same direction suggests the source analysis for this subject was not as successful – this is not implausible given the dipoles were less orthogonal for subject rj001 than rj002.

There is also a marginally significant interaction between V1 and V2 around 350ms for subject rj002, but not rj001. V2 also shows a negative going current for rj002

at 300ms for the square surround but rj001 shows no such trend except a late negative 450ms current in V2.

Discussion

The results presented support a null hypothesis that the paradigm manipulations for stimulus collinearity and stimulus surround produced effects too subtle to be detected at the field-power waveform level or did not produce any effects, but the source analysis may have supported a feedback hypothesis at the level of V1 and V2 currents. There are two major considerations to make when evaluating the results and this comes down to the contrast between the waveform modelling and the comparisons of V1 and V2 currents.

Overall, that the waveform modelling produced non-significant differences between conditions may be a reflection of the limitations of describing a waveform on the basis of signals summed from two juxtaposed areas: V1 and V2. This juxtaposition is important when considering the fact that the form completion paradigm was designed to tease apart signals on the basis of neural feedback. That differences arise once the currents are mapped to source currents for the two subjects supports the sentiment that feedback may have played a role. However, specific conclusions regarding the temporal progression of these differences is difficult given collinearity produced opposite effects for each subject for surround type. This may reflect the underlying subject variability observed in the linear modelling, reflected also in the source currents. The current variability for subjects rj001 and rj002 may also be due to the cortical patch dipoles having less than optimal dipole orthogonality. This said, it is worth acknowledging their inconsistency and a few general trends.

One main trend is that differences seem to arise most at the V2 level for the square stimulus surround (Table 3), especially for rj002. The square stimulus surround may have stimulated V2 more than V1 due to the larger RFs, though given subject

variability this is difficult to confirm. The second trend is that overall, differences for stimulus collinearity overall appear around 100ms, 250ms, and 350ms across both subjects (Table 3). Considered together, the waveform and current analysis seem to suffer from poor signal to noise ratio. However, that differences on the paradigm arise once V1 and V2 have been mapped to source currents and not at the level of field-power outlines an important point. Neural feedback between close regions like V1 and V2 may be impossible to infer at the level of summed potentials despite the form completion paradigm being developed to be sensitive to changes at that level.

The nature of the poor signal to noise ratio will be examined more closely but first examining the field topography may provide a general description of the evoked waveforms.

SVD Components

The SVD describes waveform topography by reducing the number of spatial distributions from 64 to 3.The dominant extracted component, component 1, likely corresponds to the waveform topography elicited from the stimulus paradigm. As the stimulus appeared in the top right visual field and the greatest topographic component response appeared contralateral in the lower visual field, this agrees with established understanding of the retinotopic organization of the visual cortex (Clark, et al., 1994) and supports the idea that most variation in the waveform is due to a visual cortical response.

The second and third components are similar to those reported previously (Skrandies, 1989; Skrandies & Lehmann, 1982). Skrandies and Lehmann (1982) describe component 2 to be concentrically located in a central-parietal location, and I would make a tentative comparison to our component 2. They suggest the component is related to stimulus size (Skrandies & Lehmann, 1982), though I would expand on this and suggest that given its localization to the parietal lobes may be involved with

mediating attentional effects to the hemifield as suggested by source analysis and cell recording studies that localized visual attention to that brain region (Catherine, Bushnell, & Robinson, 1981; Maeno, Gjini, Iramina, Eto, & Ueno, 2004). An alternative explanation is that this component relates to a centrally-located cortical beta rhythm that oscillates around 20Hz (Jin, Wang, & Wang, 2007; Pfurtscheller & Lopes da Silva, 1999; Scheeringa et al., 2011). The recruitment of visual attention has been repeatedly associated with a decrease in occipital alpha power and the central-beta rhythm which could be related to the 2AFC task (Ergenoglu et al., 2004; Jin, et al., 2007; Pfurtscheller & Lopes da Silva, 1999; Scheeringa, et al., 2011). Component 2 may thus be a mixture between attention-modulated parietal and beta rhythms and visual-stimulus size. However, given attention was not systematically manipulated between conditions; questions regarding attention cannot be adequately addressed. This component might provide a descriptive marker for future repeats of this paradigm.

Component 3 is likely related to the response to the elicited retinal stimulus location, component 1 (Skrandies & Lehmann, 1982), but explaining the variance associated with a secondary spread of current that spreads laterally through each brain hemisphere (Skrandies, 1989; Skrandies & Lehmann, 1982).

EEG Potentials

It would be erroneous to discuss the waveform linear models and the source analysis running t-tests in isolation of one another. As their results are in conflict, considering them together can be informative.

The variances in the linear models were poorly explained by stimulus collinearity or surround type, the experiment manipulations of interest. This was a non-significant effect across each of the time windows (100-150ms, 150-200ms, and 250-300ms). The statistically significant subject-specific effects are expected given the large subject variance in waveform amplitude leading to large amounts variance being explained by

subject in the model. The negative effect of repeat, although non-significant past 150ms, also has a clear causation given that increased time spent on visual-attention tasks increases fatigue and reduces cortical response amplitudes (Boksem, Meijman, & Lorist, 2005). That differences between vertical and horizontal forms of the stimuli were non-significant suggests if there were visual artefacts due to the CRT monitor's raster scan, these were too subtle to produce an observable neural level difference (Garcia-Perez & Peli, 2001). Pooling over the horizontal and vertical stimuli was thus appropriate for the source analysis.

The surround manipulation was designed to produce modulations on the RFs responding to the target, and this might have then allowed the inference of greater neural feedback to the square surround than to the line surround if there were differences between these conditions. On the other hand, the purpose of the collinearity manipulation was to confirm whether or not the stimulus surround condition could be tested by checking whether or not the target was actually completing the surround stimulus in the visual cortex. No significant difference in either condition would suggest that the manipulation was too subtle to produce an observable difference between conditions. I am hesitant to accept the explanation that the surround stimuli were not being integrated with target when the source analysis clearly demonstrates that differences arise when V1 and V2 are mapped to source currents (Table 3).

Given the neural response to the surround stimulus would have disappeared into background noise by 500ms (Straube & Fahle, 2010), the stimulus surround signal could only be maintained in the visual cortex through background activity and the consequent effect on the waveforms would have been small (Fingelkurts & Fingelkurts, 2006). Previous research suggests the stimulus surround may have been maintained in background neural activity through phase-locked alpha-oscillations (8-12Hz) in the visual cortex (VanRullen & Koch, 2003). Previous reports suggests such background

activity such as theta (4-8Hz) and alpha-oscillations (8-12Hz) across the parietal lobes and occipital cortex is responsible for maintaining the percept of the surround stimulus, alpha oscillations being related to tasks involving the maintenance of an internal image or expectation (Klimesch, 1999; Von Stein & Sarnthein, 2000), particularly through the phase (timing), not amplitude, of alpha oscillations (Klimesch, 2012). Time-coherent alpha oscillations observable in Figure 22 lends credibility to this idea and this aspect could be related to component 2, although not proving either case. The exact nature of the neural integration is beyond the scope of this thesis, though the use of the form completion paradigm may prove to be a useful aid in unravelling the mechanisms involved.

A possible reason that an effect would be too subtle to observe at the potential waveform level is because there were not enough subjects in the data-set to give a sufficient signal to noise ratio to detect such a difference. Alternatively, a more reasonable explanation is that the juxtaposition of V1 and V2 positive and negative going currents produces signal cancellation. Although observable noise in Figure 24 lends credence to the explanation of poor signal to noise ratio, given that significant results on the subject level were found by sourcing V1 and V2 signals in two subjects, yet there were no observable differences at the potential level across seven subjects, this suggests that current cancelation is a larger contributor to the null effect.

To look at signal to noise ratio another way, previous form perception studies using EEG reported a comparable subject number of 8 and a not so comparable 15 (Mathes, et al., 2006; Mijović, et al., 2014). Both reported large waveform differences for aligned or orthogonal form displays. As discussed previously, the large form perception waveforms from Mathes et al. and Mijović et al's studies could have arisen due to variability in stimulus displays. If they reflected genuine controlled form perception mechanisms (which is doubtful since there were so many elements on their

stimulus displays), the only reason no effect should be observed here is because controlling the display made the effect being observed small, or the dissatisfying answer of a type II error (aka. accepting a chance-occurring null hypothesis when the alternative hypothesis is true). To address the problem of signal to noise ratio, the use of more human subjects could be adopted in future. However, given the significance at the level of cortical currents it is recommended that signals be mapped to source currents across more subjects to improve the source signal clarity in V1 and V2. Emphasis should be given to the interpretation of cortical currents given signal cancelation at the potential level is possible.

V1 and V2 Interactions

The results reported above agrees with previous work that suggests the P1, 100ms waveform is associated with neural feedback from V2 to V1 (Diaz, 2013), though this effect was only observed in subject rj002. It goes contrary to a recent study that suggested the earliest feedback component to V1 must be post 150ms from the LOC (Shpaner, Molholm, Forde, & Foxe, 2013) though Shpaner et al (2013)'s study suffers from the same lack of stimulus control as others previously discussed, so their conclusions may have been premature. In line with this argument, research on illusory contours suggests the 100ms feedback projection to V1 is from the LOC (Murray et al., 2002). The current study is limited in that it is incapable of asserting what role the LOC played in this paradigm, though feedback from the LOC and V2 to V1 at 100ms is plausible. The role of the LOC in this feedback loop should be elucidated.

A 350ms interaction between V1 and V2 for the square surround stimulus suggests that if V1 and V2 signals do recurrently interact over time, it is later than the main LOC feedback projection to the early visual cortices at 300ms (Mijović, et al., 2014). Given the role of the LOC in form perception for recognising objects (Doniger et al., 2000) and the important role of feedback in integrating signals from several brain

areas (Gilbert & Li, 2013), the late V1 and V2 interaction could be influenced by feedback from this region. Such results also support the idea that feedback projections from V2 to V1 are less orientation selective than that of the RF near surround (Shushruth, et al., 2013). If this were not true, variability between the square and line surround might not be observed.

Future Directions and Implications

As discussed, source analysis combined with high resolution techniques such as fMRI and MRI is a promising technique for inferring neural feedback. As demonstrated here, when combined with controlled stimulus paradigms such as the form completion paradigm developed herein, it has the potential to produce interesting patterns of results. One of the main implications of this research is that the study of summed potentials is limited, and that inferring neural feedback on the basis of differences (or the lack thereof) at the level of neural potentials may not be possible due to current cancellation even with a paradigm developed to be sensitive to such differences.

Another key implication of this is that if a study of form perception is to inform the study of integrated brain activity by controlling RF mechanisms, the stimuli must attempt to control for these effects for the results to be meaningful. In other words, the use of whole-stimulus displays is inappropriate – this Gestalt tradition within EEG research (Wagemans, et al., 2012) should be revised if it is to make meaningful contributions beyond the field of psychology to neuroscience.

Poor signal to noise ratio in the current study is an unfortunate side effect of being unable to predict the effect of the new paradigm on neural activity, but the paradigm may still be useful in elucidating RF mechanisms of the far surround, particularly at the V1 and V2 level. In future, more subjects and data should be acquired to clarify the presented source analysis results.

A more general limitation of the source analysis method utilised is that it is restricted to those brain regions with retinotopic mapping. As one goes up in the anatomical hierarchy, the pattern of this retinotopic mapping changes, the LOC being an example of this with two purported retinotopic maps (Larsson & Heeger, 2006). Future source models will need to take into account this altered anatomy. In addition, with increasing numbers of source currents being estimated there is a risk that the estimated variance of each added area will become less accurate (Scherg & Berg, 1991). The development of new algorithms have the potential to reduce this risk (Scherg & Berg, 1991), but it poses a significant problem to the future role of functional neuroimaging research if increasing the number of regions decreases source localisation accuracy when the utility of this for mapping whole-brain activity and inter-cortical interactions is obvious.

Once the temporal contribution of neural feedback within V1 and V2 is confirmed with more data, the paradigm may be altered to investigate different aspects of form perception. For instance, giving the target disparate features to the surround such as a different colour or polarity may help investigate how these features are integrated in the cortex and how they are processed by the RF far surround.

In conclusion, this study used a novel form completion paradigm to tease apart the function of the near and far RF surround in V1. Despite the non-significant results from the waveform analysis, likely due to signal to noise ratio issues and cortical current cancellation, the fact that some differences between the stimulus conditions arose once the signals in V1 and V2 were mapped to source currents is telling, and may have important implications for the future study of form perception and neural feedback within the early visual cortices. This supports prior research suggesting a V2 to V1 feedback projection at 100ms, and adds to recent literature by making a potential LOC, V1, and V2 interaction plausible at 350ms. I hope this study highlights the importance of

neuroimaging techniques for the understanding of RF mechanisms, and that it sparks constructive debate on the utility of whole-field Gestalt form displays for the future of form perception research.

References

Ahlfors, S. P., Han, J., Belliveau, J. W., & Hämäläinen, M. S. (2010). Sensitivity of MEG and EEG to source orientation. *Brain Topography, 23*(3), 227-232.

Ahlfors, S. P., Han, J., Lin, F. H., Witzel, T., Belliveau, J. W., Hämäläinen, M. S., & Halgren, E. (2010). Cancellation of EEG and MEG signals generated by extended and distributed sources. *Human Brain Mapping, 31*(1), 140-149. doi: 10.1002/hbm.20851

Ales, J., Carney, T., & Klein, S. A. (2010). The folding fingerprint of visual cortex reveals the timing of human V1 and V2. *Neuroimage, 49*(3), 2494-2502.

Amunts, K., Malikovic, A., Mohlberg, H., Schormann, T., & Zilles, K. (2000). Brodmann's areas 17 and 18 brought into stereotaxic space—where and how variable? *Neuroimage, 11*(1), 66-84. doi: 10.1006/nimg.1999.0516

Angelucci, A., & Bressloff, P. C. (2006). Contribution of feedforward, lateral and feedback connections to the classical receptive field center and extra-classical receptive field surround of primate V1 neurons. *Progress in Brain Research, 154*, 93-120. doi: 10.1016/S0079-6123(06)54005-1

Angelucci, A., & Bullier, J. (2003). Reaching beyond the classical receptive field of V1 neurons: horizontal or feedback axons? *Journal of Physiology-Paris, 97*(2), 141-154.

Angelucci, A., Levitt, J. B., Walton, E. J., Hupe, J.-M., Bullier, J., & Lund, J. S. (2002). Circuits for local and global signal integration in primary visual cortex. *Journal of Neuroscience, 22*(19), 8633-8646.

Ary, J. P., Klein, S. A., & Fender, D. H. (1981). Location of sources of evoked scalp potentials: corrections for skull and scalp thicknesses. *Biomedical Engineering, 28*, 447-452.

Bakin, J. S., Nakayama, K., & Gilbert, C. D. (2000). Visual responses in monkey areas V1 and V2 to three-dimensional surface configurations. *Journal of Neuroscience, 20*(21), 8188-8198.

Bates, D., M, M., Bolker, B., & S, W. (2014). lme4: Linear mixed-effects models using Eigen and S4. R package version 1.1-67, from http://CRAN.R-project.org/package=lme4

Bates, D., & Maechler, M. (2014). Matrix: Sparse and Dense Matrix Classes and Methods, from http://CRAN.R-project.org/package=Matrix

Bengtsson, H. (2014). R.matlab: Read and write of MAT files together with R-to-MATLAB connectivity. Retrieved 21/0 from http://CRAN.R-project.org/package=R.matlab

Berg, P., & Scherg, M. (1994). A fast method for forward computation of multiple-shell spherical head models. *Electroencephalography and Clinical Neurophysiology, 90*(1), 58-64.

Blake, R., & Sekuler, R. (2005). *Perception* (5th ed.). New York: McGraw-Hill Higher Education.

Blakemore, C., Muncey, J. P., & Ridley, R. M. (1973). Stimulus specificity in the human visual system. *Vision Research, 13*(10), 1915-1931.

Boksem, M. A., Meijman, T. F., & Lorist, M. M. (2005). Effects of mental fatigue on attention: an ERP study. *Cognitive Brain Research, 25*(1), 107-116. doi: 10.1016/j.cogbrainres.2005.04.011

Brainard, D. H. (1997). The psychophysics toolbox. *Spatial Vision, 10*, 433-436.

Catherine, M., Bushnell, M. E. G., & Robinson, D. L. (1981). Behavioral enhancement of visual responses in monkey cerebral cortex. I. Modulation in posterior parietal cortex related to selective visual attention.

Chabre, M., & Deterre, P. (1989). Molecular mechanism of visual transduction. *European Journal of Biochemistry, 179*(2), 255-266.

Chatterjee, S., & Callaway, E. M. (2003). Parallel colour-opponent pathways to primary visual cortex. *Nature, 426*(6967), 668-671. doi: 10.1038/nature02167

Clark, V. P., Fan, S., & Hillyard, S. A. (1994). Identification of early visual evoked potential generators by retinotopic and topographic analyses. *Human Brain Mapping, 2*(3), 170-187.

Cuffin, B. N. (1998). EEG dipole source localization. *Engineering in Medicine and Biology Magazine, IEEE, 17*(5), 118-122.

Cuffin, B. N., Cohen, D., Yunokuchi, K., Maniewski, R., Purcell, C., Cosgrove, G. R., . . . Schomer, D. (1991). Tests of EEG localization accuracy using implanted sources in the human brain. *Annals of Neurology, 29*(2), 132-138. doi: 10.1002/ana.410290204

Dakin, S., & Hess, R. (1998). Spatial-frequency tuning of visual contour integration. *JOSA A, 15*(6), 1486-1499. doi: 10.1364/JOSAA.15.001486

de Graaf, T. A., & Sack, A. T. (2014). Using brain stimulation to disentangle neural correlates of conscious vision. *Consciousness Research, 5*, 1019.

DeFelipe, J., & Fariñas, I. (1992). The pyramidal neuron of the cerebral cortex: morphological and chemical characteristics of the synaptic inputs. *Progress in Neurobiology, 39*(6), 563-607.

Diaz, A. J. M. (2013). *Cortical interactions between visual areas V1 and V2 in the context of illusory contours: An electrophysiological analysis of VEPs and cortical currents in humans*. Unpublished Honours Thesis. Research School of Psychology. Australian National University. Canberra.

Dogdas, B., Shattuck, D. W., & Leahy, R. M. (2005). Segmentation of skull and scalp in 3‐D human MRI using mathematical morphology. *Human Brain Mapping, 26*(4), 273-285. doi: 10.1002/hbm.20159

Doniger, G. M., Foxe, J. J., Murray, M. M., Higgins, B. A., Snodgrass, J. G., Schroeder, C. E., & Javitt, D. C. (2000). Activation timecourse of ventral visual stream object-recognition areas: high density electrical mapping of perceptual closure processes. *J Cogn Neurosci, 12*(4), 615-621.

Dura-Bernal, S., Wennekers, T., & Denham, S. L. (2011). The role of feedback in a hierarchical model of object perception *From Brains to Systems* (pp. 165-179): Springer.

Dura-Bernal, S., Wennekers, T., & Denham, S. L. (2012). Top-down feedback in an HMAX-like cortical model of object perception based on hierarchical Bayesian networks and belief propagation. *PLoS One, 7*(11), e48216. doi: 10.1371/journal.pone.0048216

Eddelbuettel, D., & Francois, R. (2011). Rcpp: Seamless R and C++ Integration. *Journal of Statistical Software, 40*(8), 1-18.

Ergenoglu, T., Demiralp, T., Bayraktaroglu, Z., Ergen, M., Beydagi, H., & Uresin, Y. (2004). Alpha rhythm of the EEG modulates visual detection performance in humans. *Cognitive Brain Research, 20*(3), 376-383. doi: 10.1016/j.cogbrainres.2004.03.009

Felleman, D. J., & Van Essen, D. C. (1991). Distributed hierarchical processing in the primate cerebral cortex. *Cerebral Cortex, 1*(1), 1-47. doi: 10.1093/cercor/1.1.1

Ffytche, D. H., & Zeki, S. (1996). Brain activity related to the perception of illusory contours. *Neuroimage, 3*(2), 104-108. doi: 10.1006/nimg.1996.0012

Fingelkurts, A. A., & Fingelkurts, A. A. (2006). Timing in cognition and EEG brain dynamics: discreteness versus continuity. *Cognitive Processing, 7*(3), 135-162. doi: 10.1007/s10339-006-0035-0

Francis, G., & Grossberg, S. (1996). Cortical dynamics of form and motion integration: Persistence, apparent motion, and illusory contours. *Vision Research, 36*(1), 149-173. doi: 10.1016/0042-6989(95)00052-2

Garcia-Perez, M. A., & Peli, E. (2001). Luminance artifacts of cathode-ray tube displays for vision research. *Spatial Vision, 14*(2), 201-216.

Gauthier, I., Tarr, M. J., Anderson, A. W., Skudlarski, P., & Gore, J. C. (1999). Activation of the middle fusiform'face area'increases with expertise in recognizing novel objects. *Nature Neuroscience, 2*(6), 568-573.

Gegenfurtner, K. R., Kiper, D. C., & Levitt, J. B. (1997). Functional properties of neurons in macaque area V3. *Journal of Neurophysiology, 77*(4), 1906-1923.

Gerbrands, J. J. (1981). On the relationships between SVD, KLT and PCA. *Pattern recognition, 14*(1), 375-381.

Gilbert, C. D., & Li, W. (2013). Top-down influences on visual processing. *Nature Reviews Neuroscience, 14*(5), 350-363.

Goh, X. L. (2008). *Cortical Generators of Human Multifocal Visual Evoked Potentials and Fields.* Doctor of Philosophy, Australian National University, Canberra.

Gray, E. (1961). The granule cells, mossy synapses and Purkinje spine synapses of the cerebellum: light and electron microscope observations. *Journal of Anatomy, 95*(Pt 3), 345.

Hagler, D. J., Halgren, E., Martinez, A., Huang, M., Hillyard, S. A., & Dale, A. M. (2009). Source estimates for MEG/EEG visual evoked responses constrained by

multiple, retinotopically‐mapped stimulus locations. *Human Brain Mapping, 30*(4), 1290-1309. doi: 10.1002/hbm.20597

Herrmann, C. S., & Knight, R. T. (2001). Mechanisms of human attention: event-related potentials and oscillations. *Neuroscience & Biobehavioral Reviews, 25*(6), 465-476. doi: 10.1016/S0149-7634(01)00027-6

Hess, R. F., & Dakin, S. C. (1997). Absence of contour linking in peripheral vision. *Nature, 390*(6660), 602-604. doi: 10.1038/37593

Hess, R. F., & Field, D. (1999). Integration of contours: new insights. *Trends in cognitive sciences, 3*(12), 480-486.

Hirsch, J. A., & Gilbert, C. D. (1991). Synaptic physiology of horizontal connections in the cat's visual cortex. *Journal of Neuroscience, 11*(6), 1800-1809.

Hubel, D. H., & Wiesel, T. N. (1959). Receptive fields of single neurones in the cat's striate cortex. *Journal of Physiology, 148*(3), 574-591.

Hubel, D. H., & Wiesel, T. N. (1962). Receptive fields, binocular interaction and functional architecture in the cat's visual cortex. *Journal of Physiology, 160*(1), 106.

Hubel, D. H., & Wiesel, T. N. (1968). Receptive fields and functional architecture of monkey striate cortex. *Journal of Physiology, 195*(1), 215-243.

Hupe, J. M., James, A. C., Girard, P., Lomber, S. G., Payne, B. R., & Bullier, J. (2001). Feedback connections act on the early part of the responses in monkey visual cortex. *Journal of Neurophysiology, 85*(1), 134-145.

James, A. C. (2003). The pattern-pulse multifocal visual evoked potential. *Investigative Ophthalmology & Visual Science, 44*(2), 879-890. doi: 10.1167/iovs.020608

Jin, J., Wang, X., & Wang, B. (2007). *Classification of direction perception EEG Based on PCA-SVM.* Paper presented at the Natural Computation, 2007. ICNC 2007. Third International Conference on.

Johnson, R. (1993). On the neural generators of the P300 component of the event‐related potential. *Psychophysiology, 30*(1), 90-97. doi: 10.1111/j.1469-8986.1993.tb03208.x

Kanwisher, N., McDermott, J., & Chun, M. M. (1997). The fusiform face area: a module in human extrastriate cortex specialized for face perception. *Journal of Neuroscience, 17*(11), 4302-4311.

Katz, L. C., & Shatz, C. J. (1996). Synaptic activity and the construction of cortical circuits. *Science, 274*(5290), 1133-1138. doi: 10.1126/science.274.5290.1133

Kleiner, M., Brainard, D., Pelli, D., Ingling, A., Murray, R., & Broussard, C. (2007). What's new in Psychtoolbox-3. *Perception, 36*(14), 1.1-16.

Klimesch, W. (1999). EEG alpha and theta oscillations reflect cognitive and memory performance: a review and analysis. *Brain research reviews, 29*(2), 169-195.

Klimesch, W. (2012). Alpha-band oscillations, attention, and controlled access to stored information. *Trends in cognitive sciences, 16*(12), 606-617. doi: 10.1016/j.tics.2012.10.007

Lamme, V. A. F., Van Dijk, B. W., & Spekreijse, H. (1992). Texture segregation is processed by primary visual cortex in man and monkey. Evidence from VEP experiments. *Vision Research, 32*(5), 797-807. doi: 10.1016/0042-6989(92)90022-B

Larsson, J., & Heeger, D. J. (2006). Two retinotopic visual areas in human lateral occipital cortex. *The Journal of Neuroscience, 26*(51), 13128-13142. doi: 10.1523/JNEUROSCI.1657-06.2006

Lehmann, D., & Skrandies, W. (1980). Reference-free identification of components of checkerboard-evoked multichannel potential fields. *Electroencephalography and clinical neurophysiology, 48*(6), 609-621.

Light, G. A., Williams, L. E., Minow, F., Sprock, J., Rissling, A., Sharp, R., . . . Braff, D. L. (2010). Electroencephalography (EEG) and Event‐Related Potentials (ERPs) with human participants. *Current Protocols in Neuroscience,* 6.25. 21-26.25. 24.

Lopes da Silva, F. (2004). Functional localization of brain sources using EEG and/or MEG data: volume conductor and source models. *Magnetic Resonance Imaging, 22*(10), 1533-1538. doi: 10.1016/j.mri.2004.10.010

Lowel, S., & Singer, W. (1992). Selection of intrinsic horizontal connections in the visual cortex by correlated neuronal activity. *Science, 255*(5041), 209-212. doi: 10.1126/science.1372754

Luck, S. J., Woodman, G. F., & Vogel, E. K. (2000). Event-related potential studies of attention. *Trends in cognitive sciences, 4*(11), 432-440.

Machilsen, B., Novitskiy, N., Vancleef, K., & Wagemans, J. (2011). Context modulates the ERP signature of contour integration. *PLoS One, 6*(9), e25151.

Maeno, T., Gjini, K., Iramina, K., Eto, F., & Ueno, S. (2004). *Event-related potential P2 derived from visual attention to the hemi-space. Source localization with LORETA.* Paper presented at the International Congress Series.

Maffei, L., Fiorentini, A., & Bisti, S. (1973). Neural correlate of perceptual adaptation to gratings. *Science, 182*(4116), 1036-1038. doi: 10.1126/science.182.4116.1036

Mathes, B., Trenner, D., & Fahle, M. (2006). The electrophysiological correlate of contour integration is modulated by task demands. *Brain research, 1114*(1), 98-112. doi: 10.1016/j.brainres.2006.07.068

MATLAB and Statistics Toolbox Release 2012b, The MathWorks, Inc., Natick, Massachusetts, United States.

McGuire, B. A., Gilbert, C. D., Rivlin, P. K., & Wiesel, T. N. (1991). Targets of horizontal connections in macaque primary visual cortex. *Journal of Comparative Neurology, 305*(3), 370-392. doi: 10.1002/cne.903050303

McLoughlin, N., & Schiessl, I. (2006). Orientation selectivity in the common marmoset (< i> Callithrix jacchus</i>): The periodicity of orientation columns in V1 and V2. *Neuroimage, 31*(1), 76-85. doi: 10.1016/j.neuroimage.2005.12.054

Michel, C. M., & Murray, M. M. (2012). Towards the utilization of EEG as a brain imaging tool. *NeuroImage, 61*(2), 371-385. doi: 10.1016/j.neuroimage.2011.12.039

Mijović, B., De Vos, M., Vanderperren, K., Machilsen, B., Sunaert, S., Van Huffel, S., & Wagemans, J. (2014). The dynamics of contour integration: A simultaneous EEG–fMRI study. *Neuroimage, 88*, 10-21. doi: 10.1016/j.neuroimage.2013.11.032

Mikami, A., Newsome, W. T., & Wurtz, R. H. (1986). Motion selectivity in macaque visual cortex. I. Mechanisms of direction and speed selectivity in extrastriate area MT. *Journal of Neurophysiology, 55*(6), 1308-1327.

Murray, M. M., Wylie, G. R., Higgins, B. A., Javitt, D. C., Schroeder, C. E., & Foxe, J. J. (2002). The spatiotemporal dynamics of illusory contour processing: combined high-density electrical mapping, source analysis, and functional magnetic resonance imaging. *The Journal of Neuroscience, 22*(12), 5055-5073.

Nugent, A. K., Keswani, R. N., Woods, R. L., & Peli, E. (2003). Contour integration in peripheral vision reduces gradually with eccentricity. *Vision Research, 43*(23), 2427-2437. doi: 10.1016/S0042-6989(03)00434-6

Ölveczky, B. P., Baccus, S. A., & Meister, M. (2003). Segregation of object and background motion in the retina. *Nature, 423*(6938), 401-408. doi: 10.1038/nature01652

Pfurtscheller, G., & Lopes da Silva, F. H. (1999). Event-related EEG/MEG synchronization and desynchronization: basic principles. *Clinical Neurophysiology, 110*(11), 1842-1857.

Pizzagalli, D. A. (2007). Electroencephalography and high-density electrophysiological source localization *Handbook of Psychophysiology* (Vol. 3, pp. 56-84).

Pruis, G., Gilding, B. H., & Peters, M. (1993). A comparison of different numerical methods for solving the forward problem in EEG and MEG. *Physiological measurement, 14*(4A), A1.

Ramon, C., Schimpf, P. H., & Haueisen, J. (2006). Influence of head models on EEG simulations and inverse source localizations. *BioMedical Engineering Online, 5*(1), 10. doi: 10.1186/1475-925X-5-10

Rees, G. (2007). Neural correlates of the contents of visual awareness in humans. *Philosophical Transactions of the Royal Society B: Biological Sciences, 362*(1481), 877-886. doi: 10.1098/rstb.2007.2094

Roe, A. W. (2011). Functional connectivity of color and form in V1 and V2. *Journal of Vision, 11*(15). doi: 10.1167/11.15.21

Roe, A. W., Chelazzi, L., Connor, C. E., Conway, B. R., Fujita, I., Gallant, J. L., . . . Vanduffel, W. (2012). Toward a unified theory of visual area V4. *Neuron, 74*(1), 12-29. doi: 10.1016/j.neuron.2012.03.011

Roe, A. W., & Daniel, Y. (1999). Specificity of color connectivity between primate V1 and V2. *Journal of Neurophysiology, 82*(5), 2719-2730.

Rush, S., & Driscoll, D. A. (1968). Current distribution in the brain from surface electrodes. *Anesthesia & Analgesia, 47*(6), 717-723.

Sarkar, D. (2008). *Lattice: Multivariate Data Visualization with R*. New York: Springer.

Scheeringa, R., Fries, P., Petersson, K.-M., Oostenveld, R., Grothe, I., Norris, D. G., . . . Bastiaansen, M. (2011). Neuronal dynamics underlying high-and low-frequency EEG oscillations contribute independently to the human BOLD signal. *Neuron, 69*(3), 572-583.

Scherg, M., & Berg, P. (1991). Use of prior knowledge in brain electromagnetic source analysis. *Brain Topography, 4*(2), 143-150.

Schiller, P. H., & Malpeli, J. G. (1978). Functional specificity of lateral geniculate nucleus laminae of the rhesus monkey. *Journal of Neurophysiology, 41*(3), 788-797.

Schira, M. M., Wade, A. R., & Tyler, C. W. (2007). Two-dimensional mapping of the central and parafoveal visual field to human visual cortex. *Journal of Neurophysiology, 97*(6), 4284-4295. doi: 10.1152/jn.00972.2006

Shani, R., & Sagi, D. (2005). Eccentricity effects on lateral interactions. *Vision Research, 45*(15), 2009-2024. doi: 10.1016/j.visres.2005.01.024

Shigihara, Y., & Zeki, S. (2014). Parallel processing in the brain's visual form system: An fMRI study. *Name: Frontiers in Human Neuroscience, 8*, 506. doi: 10.3389/fnhum.2014.00506

Shpaner, M., Molholm, S., Forde, E., & Foxe, J. J. (2013). Disambiguating the roles of area V1 and the lateral occipital complex (LOC) in contour integration. *Neuroimage, 69*, 146-156.

Shushruth, S., Nurminen, L., Bijanzadeh, M., Ichida, J. M., Vanni, S., & Angelucci, A. (2013). Different orientation tuning of near-and far-surround suppression in macaque primary visual cortex mirrors their tuning in human perception. *Journal of Neuroscience, 33*(1), 106-119. doi: 10.1523/JNEUROSCI.2518-12.2013

Sincich, L. C., & Horton, J. C. (2002). Divided by cytochrome oxidase: a map of the projections from V1 to V2 in macaques. *Science, 295*(5560), 1734-1737.

Sincich, L. C., & Horton, J. C. (2005). The circuitry of V1 and V2: Integration of color, form, and motion. *Annual Review of Neuroscience, 28*, 303-326. doi: 10.1146/annurev.neuro.28.061604.135731

Sincich, L. C., Jocson, C. M., & Horton, J. C. (2010). V1 interpatch projections to V2 thick stripes and pale stripes. *Journal of Neuroscience, 30*(20), 6963-6974. doi: 10.1523/JNEUROSCI.5506-09.2010

Skrandies, W. (1989). Data reduction of multichannel fields: Global field power and principal component analysis. *Brain topography, 2*(1-2), 73-80.

Skrandies, W. (1990). Global field power and topographic similarity. *Brain topography, 3*(1), 137-141.

Skrandies, W., & Lehmann, D. (1982). Spatial principal components of multichannel maps evoked by lateral visual half-field stimuli. *Electroencephalography and clinical neurophysiology, 54*(6), 662-667.

Straube, S., & Fahle, M. (2010). The electrophysiological correlate of saliency: evidence from a figure-detection task. *Brain research, 1307*, 89-102. doi: 10.1016/j.brainres.2009.10.043

Straube, S., Grimsen, C., & Fahle, M. (2010). Electrophysiological correlates of figure–ground segregation directly reflect perceptual saliency. *Vision Research, 50*(5), 509-521. doi: 10.1016/j.visres.2009.12.013

Team, R. C. (2014). R: A language and environment for statistical computing., 2014, from http://www.R-project.org/

Ungerleider, L. G., & Desimone, R. (1986). Cortical connections of visual area MT in the macaque. *Journal of Comparative Neurology, 248*(2), 190-222.

Van Essen, D. C., Anderson, C. H., & Felleman, D. J. (1992). Information processing in the primate visual system: an integrated systems perspective. *Science, 255*(5043), 419-423.

Vanni, S., Henriksson, L., & James, A. (2005). Multifocal fMRI mapping of visual cortical areas. *Neuroimage, 27*(1), 95-105. doi: 10.1016/j.neuroimage.2005.01.046

VanRullen, R., & Koch, C. (2003). Is perception discrete or continuous? *Trends in Cognitive Sciences, 7*(5), 207-213. doi: 10.1016/S1364-6613(03)00095-0

von der Heydt, R., & Peterhans, E. (1989). Mechanisms of contour perception in monkey visual cortex. I. Lines of pattern discontinuity. *Journal of Neuroscience, 9*(5), 1731-1748.

Von Stein, A., & Sarnthein, J. (2000). Different frequencies for different scales of cortical integration: from local gamma to long range alpha/theta synchronization. *International Journal of Psychophysiology, 38*(3), 301-313.

Wagemans, J., Elder, J. H., Kubovy, M., Palmer, S. E., Peterson, M. A., Singh, M., & von der Heydt, R. (2012). A century of Gestalt psychology in visual perception: I. Perceptual grouping and figure–ground organization. *Psychological bulletin, 138*(6), 1172. doi: 10.1037/a0029333

Weliky, M., Kandler, K., Fitzpatrick, D., & Katz, L. C. (1995). Patterns of excitation and inhibition evoked by horizontal connections in visual cortex share a common relationship to orientation columns. *Neuron, 15*(3), 541-552. doi: 10.1016/0896-6273(95)90143-4

Wickham, H. (2007). Reshaping data with the reshape package. *Journal of Statistical Software, 21*(12), 2007.

Wokke, M. E., Vandenbroucke, A. R., Scholte, H. S., & Lamme, V. A. (2012). Confuse your illusion feedback to early visual cortex contributes to perceptual

completion. *Psychological science*, 0956797612449175. doi: 10.1177/0956797612449175

Yau, J. M., Pasupathy, A., Brincat, S. L., & Connor, C. E. (2013). Curvature processing dynamics in macaque area V4. *Cerebral Cortex, 23*(1), 198-209. doi: 10.1093/cercor/bhs004

Footnotes

[1.] From "Texture segregation is processed by primary visual cortex in man and monkey. Evidence from VEP experiments." by Lamme, V. A. F., Van Dijk, B. W., and Spekreijse, H., 1992, *Vision Research*, 32(5), 797-807. doi: 10.1016/0042-6989(92)90022-B. Copyright 2015 by Elsevier. Permission conveyed through Copyright Clearance Center, Inc.

[2.] From "Integration of contours: new insights." by Hess, R. F., and Field, D., 1999, *Trends in cognitive sciences*, 3(12), 480-486. Copyright 2015 by Elsevier. Permission conveyed through Copyright Clearance Center, Inc.

[3.] From "Brain activity related to the perception of illusory contours." by Ffytche, D. H., and Zeki, S., 1996, *Neuroimage*, 3(2), 104-108. doi: 10.1006/nimg.1996.0012. Copyright 2015 by Elsevier. Permission conveyed through Copyright Clearance Center, Inc.

[4.] From "Different orientation tuning of near-and far-surround suppression in macaque primary visual cortex mirrors their tuning in human perception." by Shushruth, S., Nurminen, L., Bijanzadeh, M., Ichida, J. M., Vanni, S., and Angelucci, A., 2013, *Journal of Neuroscience*, 33(1), 106-119. doi: 10.1523/JNEUROSCI.2518-12.2013. Copyright 2015 by the Journal of NEuroscience. Permission conveyed through Copyright Clearance Center, Inc.

[5.] From "Multifocal fMRI mapping of visual cortical areas." by Vanni, S., Henriksson, L., and James, A., 2005, *Neuroimage*, 27(1), 95-105. doi: 10.1016/j.neuroimage.2005.01.046. Copyright 2015 by Elsevier. Permission conveyed through Copyright Clearance Center, Inc.

[6.] From "Brodmann's areas 17 and 18 brought into stereotaxic space—where and how variable?" by Amunts, K., Malikovic, A., Mohlberg, H., Schormann, T., and Zilles, K., 2000, *Neuroimage*, 11(1), 66-84. doi: 10.1006/nimg.1999.0516. Copyright 2015 by Elsevier. Permission conveyed through Copyright Clearance Center, Inc.

[7.] From "*Cortical Generators of Human Multifocal Visual Evoked Potentials and Fields.*" by Goh, X. L., 2008, Doctor of Philosophy, Australian National University, Canberra. Copyright permission obtained in 2015 from author.